

NPS ARCHIVE

1961

TSO, L.

A STUDY OF FRICTION LOSS
FOR SPUR GEAR TEETH

LU-NIEN TSO

LIBRARY
U.S. NAVAL POSTGRADUATE SCHOOL
MONTEREY, CALIFORNIA

A STUDY OF FRICTION LOSS
FOR
SPUR GEAR TEETH

* * * * *

Tso, Lu-nien

A STUDY OF FRICTION LOSS
FOR
SPUR GEAR TEETH

by

Tso, Lu-nien
//
Lieutenant, Chinese Navy

Submitted in partial fulfillment of
the requirements for the degree of

MASTER OF SCIENCE
IN
MECHANICAL ENGINEERING

United States Naval Postgraduate School
Monterey, California

1961

NPC Archive

2022

961

Tso, L.

80

1990-1991

80

1990-1991

80

1990-1991

80

1990-1991

80

1990-1991

80

1990-1991

80

1990-1991

80

1990-1991

80

Library
U. S. Naval Postgraduate School
Monterey, California

A STUDY OF FRICTION LOSS

FOR

SPUR GEAR TEETH

by

Tso, Lu-nien

This work is accepted as fulfilling
the thesis requirements for the degree of

MASTER OF SCIENCE

IN

MECHANICAL ENGINEERING

from the

United States Naval Postgraduate School

ABSTRACT

In this thesis, the power loss due to the mating gear tooth profile surfaces sliding on each other is determined analytically by using the basic consideration that the power loss is the product of the frictional force and the relative sliding velocity of the mating gear teeth.

The frictional force is related to the normal load applied on the tooth surfaces and the coefficient of friction between them. The relative sliding velocity is related to the curvature of the tooth profile.

The load distribution, when more than one pair of teeth are in contact, is determined by systematic analysis from the empirical formula based on H. Walker's experimental results of spur gear tooth deflections. The results are compared with the results when the tooth is considered rigid, and also with the results obtained by H. E. Merritt, for a particular case with a different method of approach.

The value of the coefficient of friction is selected by judging the values suggested and the published experimental test data available.

The methods for determining the efficiency of gears are given in the general cases. A chart of the tooth loss factor for standard 20° full-depth teeth is plotted.

The power loss calculated in this thesis is compared with that of the actual test data for a gear box unit designed, manufactured, and tested by Western Gear Corporation. A close agreement between the calculated results and the test data is shown.

TABLE OF CONTENTS

Article	Title	Page
I.	Introduction	1
II.	Relative Sliding Velocity of Mating Teeth	3
III.	Contact Ratio	7
IV.	Gear Tooth Loading	11
V.	Power Loss	27
VI.	Coefficient of Friction	40
VII.	Efficiency	42
VIII.	Effect of Manufacturing Error	49
IX.	Practical Example	53
X.	Conclusions	56
	Bibliography	59
Appendix I.	Sample Calculations of Gear Tooth Load Distribution	60
Appendix II.	Comparison of Friction Loss Due to Tooth Sliding	64
Appendix III.	Detail Calculations on the Practical Example	66

LIST OF ILLUSTRATIONS

Figure	Page
1. Relative Sliding Velocity Distribution Diagram for External Gear Mesh	4
2. Internal Mesh	5
3. Contact Ratio	8
4. Maximum Length of Line of Action	8
5. Contact Ratio Range of $14 \frac{1}{2}^\circ$ Full-depth Teeth	10
6. Load Distribution on Rigid Teeth	11
7. Derivation of Gear Tooth Deflection	13
8. Governing Variables of Tooth Deflection	15
9. Relation of Load Applied Angle for Both Pinion and Gear Showing Separately, When Two Pairs of Teeth are in Contact	16
10. Root Thickness When $d_r > d_b$	20
11. Root Thickness When $d_r < d_b$	20
12. Load Distribution of Elastic Teeth	21
13. Load Distribution on the Recess Side of Line of Action of 20° Full-depth Teeth	23
14. Load Distribution on the Recess Side of Line of Action of 20° Full-depth Teeth	24
15. Load Distribution on the Recess Side of Line of Action of 20° Full-depth Teeth	25
16. Load Distribution on the Recess Side of Line of Action of 20° Full-depth Teeth	26
17. Power Loss Diagram and Cycles for Rigid Tooth When $1 < m_p < 2$; $p_b > Z_a$; $p_b > Z_r$	28
17a. Power Loss Diagram and Cycles for Rigid Tooth When $1 < m_p < 2$; $p_b < Z_a$; $p_b > Z_r$	29
18. Power Loss Diagram and Cycles for Elastic Tooth When $1 < m_p < 2$; $p_b > Z_a$; $p_b > Z_r$	32

	Page
19. Power Loss Diagram and Cycles for Rigid Tooth When $2 < m_p < 3$; $Z_a > p_b$; $Z_r > p_b$	35
19a. Power Loss Diagram and Cycles for Rigid Tooth When $2 < m_p < 3$; $Z_a > p_b$; $Z_r < p_b$	36
20. Tooth Loss Factor of 20° Full-depth Spur Gear	46
21. Comparison of Tooth Loss Factor of 20° Full-depth Spur Gear with the Results Developed by Merritt Shown in Dotted Line.	47
22. Load Distribution Diagram for Rigid Tooth When Deviation in Profile or Spacing Occurs	50
23. General Arrangement of a Practical Gear Box Unit	53

Table

1. Comparison of Friction Loss of Rigid Teeth and Elastic Teeth	34
2. Comparison of Gear Tooth Friction Loss Based on Merritt's Equation	48
3. Summary of the Effect of Uniform Manufacturing Error	52

LETTER SYMBOLS

(A) Gears

a	addendum
a_g	addendum of gear
a_p	addendum of pinion
C	center distance
c	clearance
b_g	dedendum of gear
b_p	dedendum of pinion
h	height, depth
h_r	working depth
h_t	whole depth (total depth)
D	pitch diameter of gear
d	pitch diameter of pinion
D_o	outside diameter of gear
d_o	outside diameter of pinion
D_b	base diameter of gear
d_b	base diameter of pinion
D_r	root diameter of gear
d_r	root diameter of pinion
s	distance, linear or along an arc
θ	distance, angular (angle in polar coordinates)
F	face width
K, k	factor, constant
L, l	lengths
Z	length of line of action
Z_a	approach portion of line of action

Z_r	recess portion of line of action
W	load (total)
w	load per tooth
N	number of teeth
N_g	number of teeth in gear
N_p	number of teeth in pinion
p	pitch, circular
P_b	base pitch (normal to involute)
P_d	pitch, diametral
P_f	instantaneous power, friction
P_f	power, friction
ϕ	pressure angle
R	pitch radius of gear
r	pitch radius of pinion
R_b	base radius of gear
r_b	base radius of pinion
R_o	outside radius of gear
r_o	outside radius of pinion
R_r	root radius of gear
r_r	root radius of pinion
P	radius of curvature
P_g	profile radius of curvature in gear
P_p	profile radius of curvature in pinion
m_g	gear ratio
m_p	contact ratio
n	revolutions per unit time
t	thickness

t_g	circular thickness of gear
t_p	circular thickness of pinion
t_c	chordal thickness
v	velocity, linear
ω	velocity, angular
ω_g	angular velocity of gear
ω_p	angular velocity of pinion
Δ	tooth loss factor
δ	gear tooth deflection
λ	combined stiffness
μ	coefficient of friction

(B) Miscellaneous:

A	area
c	clearance, diametral
D	diameter
d	diameter
F	force
H	power loss
j	power loss coefficient
L	length
M	power loss per square inch
N	revolutional speed
P	pressure
R	reaction force
S	Sommerfeld number
T	temperature
U	speed, linear
W	weight
Z	viscosity

I. Introduction

In the field of gear design, power losses are an important consideration. One of the power losses is due to the mating gear tooth profile surfaces sliding on each other, the direction being tangent to the tooth profile with varying magnitude along the line of action. Whenever a sliding motion exists between two surfaces with a normal load applied, there must be a certain amount of frictional force exerted. This frictional force causes friction power loss when gears are operating.

The power loss due to gear tooth ~~sliding~~ can be determined from the work done per unit time by the frictional force. The basic consideration of this friction power loss is the product of the frictional force and the sliding velocity. The frictional force depends upon the normal load applied on the tooth at the point of contact and the coefficient of friction between them. The sliding velocity turns out to be a function of the curvatures of the tooth profiles at the point of contact. Thus, the normal load applied on gear teeth, the coefficient of friction, and the relative sliding velocity are the significant factors which will govern the power loss, and alternatively, they also govern the efficiency.

The analytic approach to this problem is then to analyze those factors based on the theoretical and experimental results available. The normal load is related to the number of teeth in contact (contact ratio) and to the tooth deflection. The only tooth deflection data found during this study are those experimental results for spur gears obtained by H. Walker. [5] Therefore, the determination of power loss and efficiency due to gear tooth sliding will be confined to spur gears.

*Numbers in brackets refer to number of reference in the Bibliography ., 50.

The determination of power loss and efficiency of spur gears has been made by H. E. Merritt ^[1] by a different approach, but his results hold only for a particular case.

In this thesis, standard involute tooth forms are analyzed systematically. A general method is obtained, and it can also be applied to other specially modified teeth of involute form in order to determine the power loss and the efficiency of the modified teeth.

The effect of manufacturing error on power loss is considered and related to the length of approach and the length of recess.

II. Relative Sliding Velocity of Mating Teeth

Fig. 1 shows a pair of external involute teeth mating with each other. Their contact begins at i proceeds along the line of action passing through pitch point o , and separates at e . By the principle of mechanisms, the pitch point is the only point that the teeth on both the gear and the pinion have the same velocity. At any point of contact which is not on the line of centers of the gear and pinion, relative velocity will occur. Therefore, within this line of action, curved tooth surfaces move across one another with a combination of rolling and sliding motion. The motion of sliding is the motion which causes most of the power loss.

If the contact point is at any point x within the line of action, the relative sliding velocity^[3] is the difference of the instantaneous velocity of the contact point x on the pinion and gear.

$$V = P_p \omega_p - P_g \omega_g \quad (1)$$

By introducing the relations

$$P_g = C \sin \phi - P_p$$

$$\omega_g = \frac{\omega_p}{m_g}$$

Eq. (1) can be simplified to

$$V = (P_p - r \sin \phi) \left(\frac{m_g + 1}{m_g} \right) \omega_p$$

where $P_p - r \sin \phi$ is the distance \overline{ox} of contact point x from the pitch point o along the line of action. It can be positive or negative in sign, depending upon which side of pitch point, the contact point is located.

For power loss calculation, we are interested only in the magnitude of this relative velocity.

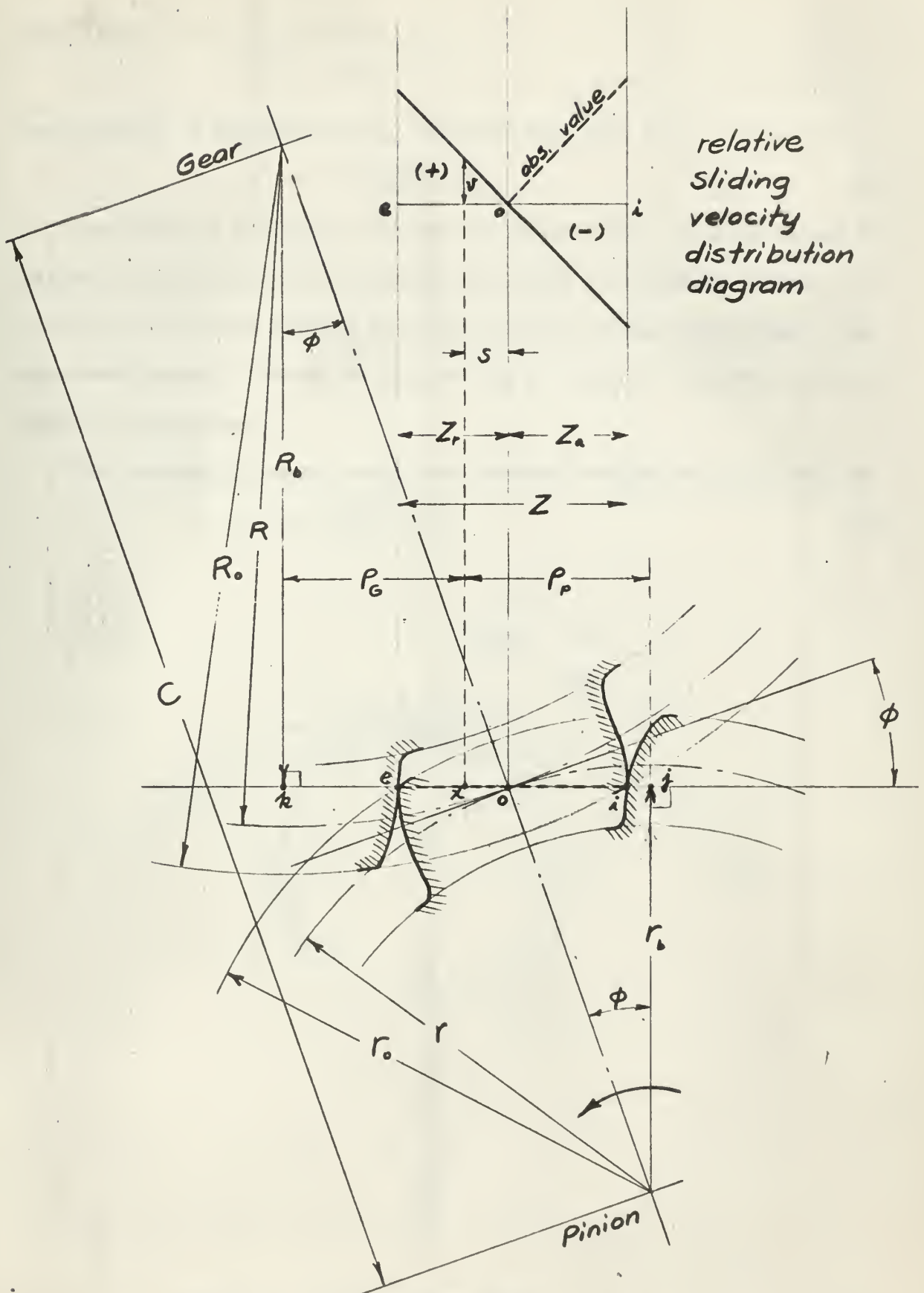


Fig. 1. Relative sliding velocity distribution diagram for external gear mesh

Then, let

$$|P_p - r \sin \phi| = s$$

the equation of relative sliding velocity will then be

$$v = s \left(\frac{m_g + 1}{m_g} \right) \omega_p \quad (2)$$

For gears in operation with the teeth under load, a small amount of deflection will occur. This changes the radii of curvature P_p and P_g , so that the relative sliding velocity will also change accordingly, but this small amount of tooth deflection can be neglected compared to the radius of curvature.

For internally meshed teeth, the relative sliding velocity will be

$$v = s \left(\frac{m_g - 1}{m_g} \right) \omega_p \quad (3)$$

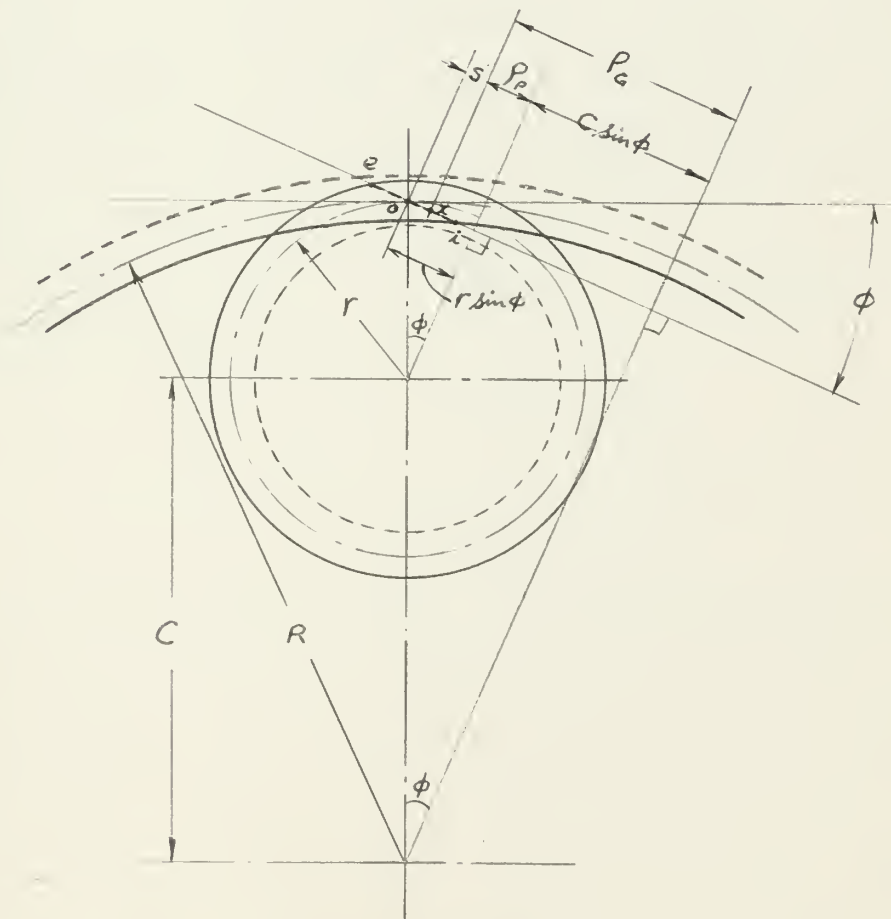


Fig. 2, Internal gear mesh

Equation (3) can be derived from Fig. 2 where $P_g = C \sin \phi + P_p$

Equations (2) and (3) show that the relative sliding velocity is a linear function of the distance of point of contact from the pitch point.

III. Contact Ratio

The contact ratio is defined^[7] as the ratio of the length of the line of contact to the base pitch and is denoted by m_p ; thus for the gear shown in Fig. 3

$$m_p = \frac{Z}{P_b} = \frac{Z_a + Z_r}{P_b} \quad (4)$$

Referring to Fig. 1 the contact ratio can be expressed as

$$m_p = \frac{\sqrt{R_o^2 - R_b^2} + \sqrt{r_o^2 - r_b^2} - c \sin \phi}{\left(\frac{\pi \cos \phi}{P_d} \right)} \quad (5)$$

where $P_b = p \cos \phi = \frac{\pi \cos \phi}{P_d}$

For standard full-depth teeth the addendum, $a = \frac{l}{P_d}$, but from the expression of Eq. (5) it is difficult to see what will be the range of the contact ratio. If we increase the radii of the gear and the pinion until they approach infinity, the gears in Fig. 3 become two racks as shown in Fig. 4. In this limiting case, the line of contact has the maximum possible length and the maximum contact ratio will be

$$(m_p)_{\max.} = \frac{Z_{\max.}}{P_b} = \frac{\left(\frac{2a}{\sin \phi} \right)}{\left(\frac{\pi \cos \phi}{P_d} \right)} = \frac{4}{\pi \sin 2\phi}$$

For standard full-depth teeth:

$$14\frac{1}{2}^\circ \text{ teeth} \quad (m_p)_{\max.} = 2.63$$

$$20^\circ \text{ teeth} \quad (m_p)_{\max.} = 1.98$$

$$25^\circ \text{ teeth} \quad (m_p)_{\max.} = 1.66$$

For actual gear pairs, the contact ratio will never reach the value as listed above, because two racks meshed with one another does not constitute gear action. Thus, we can easily see that for 20° and 25° standard full-depth teeth, the contact ratio will be never greater than 2. In other words, the load is always carried by 1 or 2 pairs of teeth. For $14\frac{1}{2}^\circ$ standard full-depth teeth, the gear action in some cases will be alternatively carried by 2 and 3 pairs of teeth, and in some other cases if the

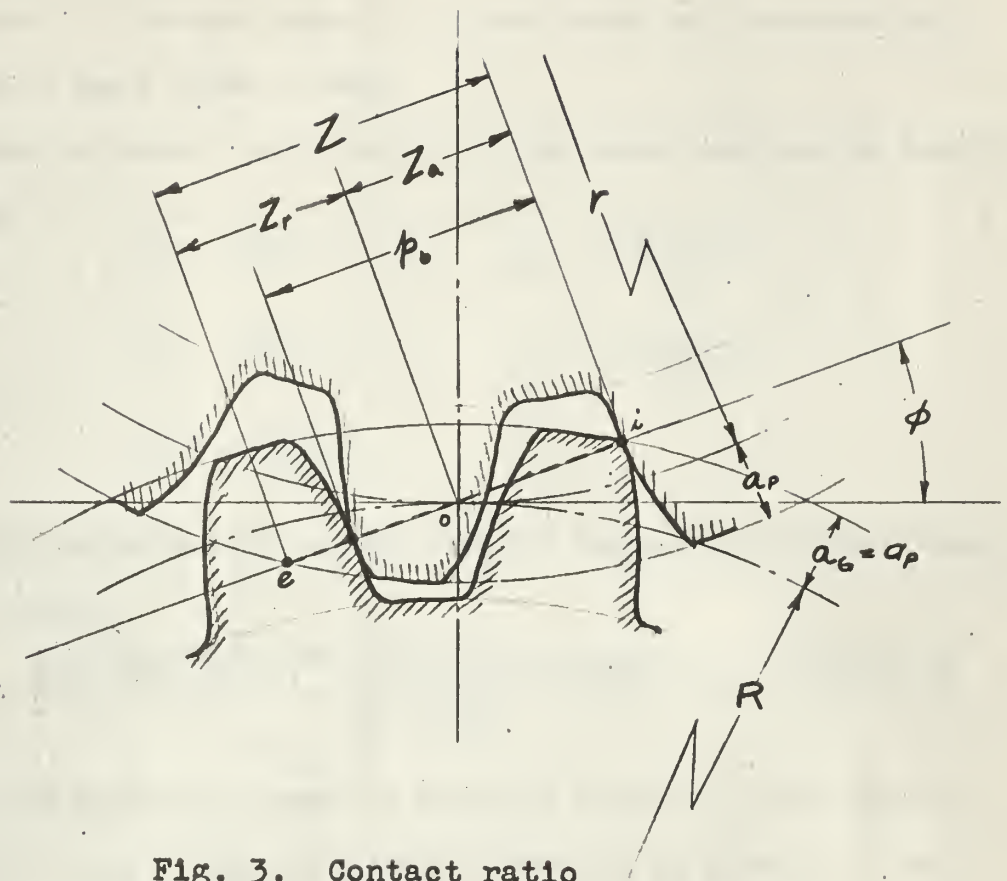


Fig. 3. Contact ratio

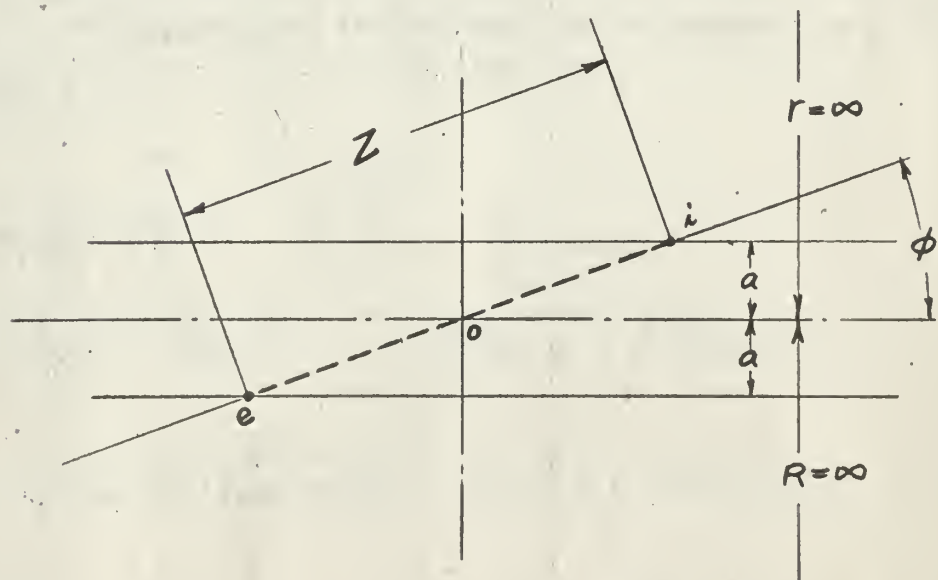


Fig. 4. Maximum length of line of action

radii of gear and pinion decrease to a certain value (or the number of teeth decrease to a certain number), the gear action will alternatively be carried by 1 and 2 pairs of teeth.

The range of contact ratio for $14\frac{1}{2}^\circ$ full-depth teeth can be found by substituting

$$D_o = \frac{N_G + 2}{P_d} \quad ; \quad D_b = \frac{N_G \cos \phi}{P_d}$$

$$d_o = \frac{N_p + 2}{P_d} \quad ; \quad d_b = \frac{N_p \cos \phi}{P_d}$$

$$p_o = \frac{\pi \cos \phi}{P_d}$$

into Eq. (5); then we get the contact ratio m_p expressed in terms of number of teeth N_G and N_p ,

$$m_p = \frac{\sqrt{(N_G + 2)^2 - (N_G \cos \phi)^2} + \sqrt{(N_p + 2)^2 - (N_p \cos \phi)^2} - (N_p + N_G) \sin \phi}{2 \pi \cos \phi}$$

By substituting different numbers of teeth for N_p and N_G , the range of contact ratio m_p can be plotted against N_p and N_G , as in Fig. 5. The shaded area indicates that interference will occur, and the relation of N_p and N_G for the beginning of interference can be expressed as follows, referring Fig. 1

$$\text{if } \overline{o_i} = \overline{o_j}$$

$$\sqrt{\left(\frac{D_o}{2}\right)^2 - \left(\frac{D_b}{2}\right)^2} - \frac{D}{2} \sin \phi = \frac{d}{2} \sin \phi$$

$$\frac{1}{2} \sqrt{\left(\frac{N_G + 2}{P_d}\right)^2 - \left(\frac{N_G \cos \phi}{P_d}\right)^2} - \frac{1}{2} \frac{N_G \sin \phi}{P_d} = \frac{1}{2} \frac{N_p}{P_d} \sin \phi$$

$$\therefore \sqrt{(N_G + 2)^2 - (N_G \cos \phi)^2} - N_G \sin \phi = N_p \sin \phi$$

IV. Gear Tooth Loading

It has been found in the previous article that the contact ratio for most practical cases lies between 1 and 2, that is the gear action is alternatively carried by 1 and 2 pairs of teeth, except some gear teeth combinations of $14\frac{1}{2}^{\circ}$ full-depth teeth have the contact ratio between 2 and 3.

When two pairs of teeth are in contact, if the teeth were perfectly rigid, there would be an equal distribution of load, each carrying half the load, as shown in Fig. 6.

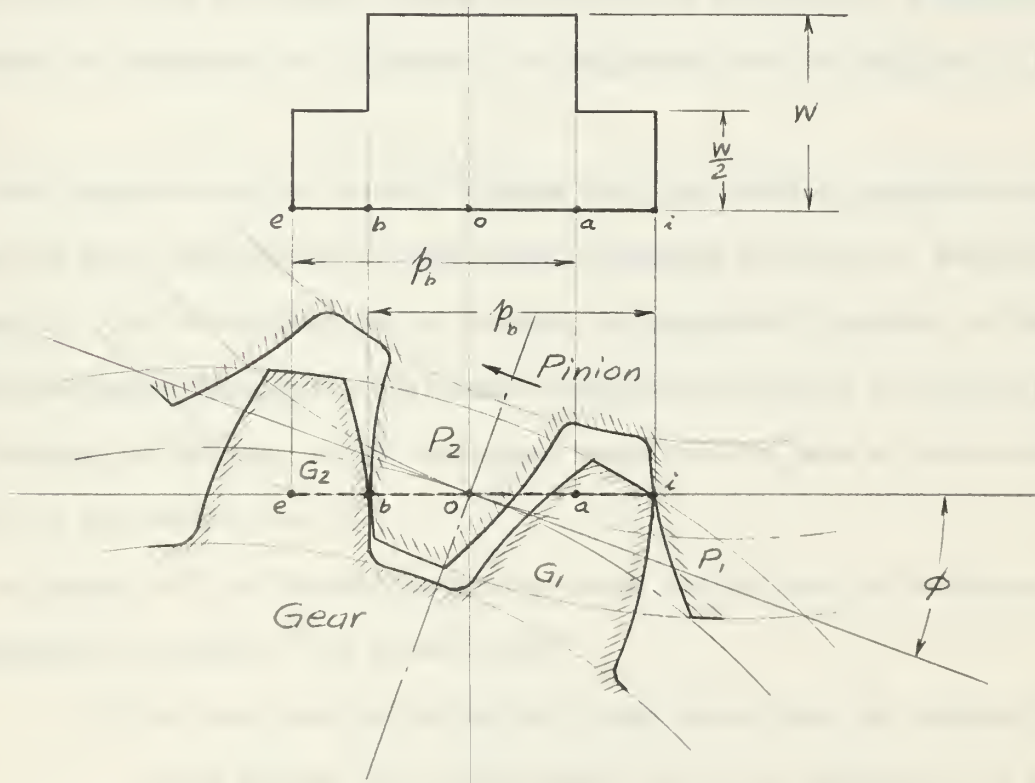


Fig. 6 Load distribution on rigid teeth.

The deflection of elastic teeth causes a change of load distribution. When two pairs of teeth are in contact, the sum of the deflections of the first pair must be equal to the sum of the deflections of the second pair.

A gear tooth subjected to a load acting normal to the surface and in the direction of the line of action is subjected to two types of deflections, these are:-

- (a) A displacement of the tooth due to bending and compression deflection and to shear deflection.
- (b) A depression or deformation of the surface round about the theoretical point of contact due to the surface compression of the tooth.

Owing to the complication of numerous factors which control the total deflection caused by bending, shear, compression and surface deformation, it would be impossible to calculate its magnitude with any degree of simplicity.

Test results made by Walker^[4] shows that the testing experiment measures the total deflection of the tooth, including that due to surface deformation. The deflection due to surface deformation is capable of being calculated approximately, and although comparatively small in proportion to the bending deflection, is of sufficient magnitude to have an appreciable effect on the tooth load.

A summary of the factors governing tooth deflection, as determined experimentally by Walker^[4] is given below:-

- (1) For any gear subjected to a load which does not stress the teeth beyond the proportional limit, the deflection is proportional to the load.
- (2) The deflection under a given load is independent of the pitch: in other words, gears of similar proportions (i.e., of the same number of teeth and the same pressure angle), but of different pitches, deflect equal amounts when subjected to

the same load applied at similar points.

(3) The deflection due to surface deformation at the point of contact is dependent only on the load, and is essentially independent of the number of teeth and relative curvature of the gear teeth. The deflection due to surface deformation is small compared with that due to bending and shear, so that the approximation involved is close enough for all practical purposes.

(4) The magnitude of the deflection varies with different tooth shapes (numbers of teeth and pressure angle); in general, the deflection decreases with an increase in the number of teeth, as would be expected.

From the test results made by Walker,^[5] an empirical formula has been evolved having a mathematical basis approximating to required conditions. Referring to Fig. 7, it has been stated that the magnitude of the deflection is independent of the pitch, and consequently it would be expected

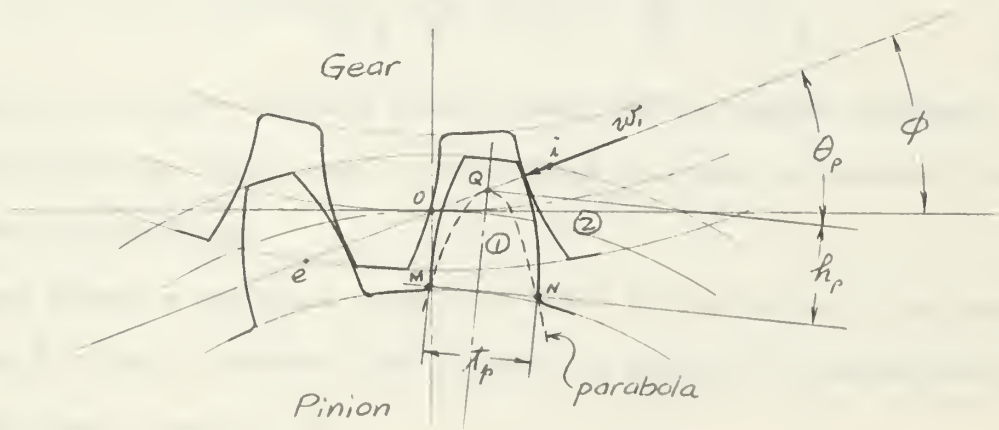


Fig. 7. Derivation of gear tooth deflection

that the deflection would be proportional to some function of the ratio $\frac{h}{t}$. An analogous case is that of a cantilever of unit width and of length h and thickness t ; the deflection due to bending is dependent only on the load and a function of the ratio $\frac{h}{t}$, for compression and shear deflection it can be shown that the same rule holds good, and that the deflection is proportional to the ratio of $\frac{h}{t}$. Then the deflection of tooth 1 on pinion will be

$$\delta_p = K \frac{w_r}{E} \cdot \frac{h_p}{t_p} \cos \theta_p \quad (6)$$

where w_r = load normal to the involute at one of the contact points

E = modulus of elasticity

K = constant of experiment

h_p = depth, referring to Fig. 7

t_p = thickness, referring to Fig. 7

θ_p = load angle, referring to Fig. 7

Similarly, the deflection of mating tooth 2 on gear will be

$$\delta_g = K \frac{w_r}{E} \cdot \frac{h_g}{t_g} \cos \theta_g \quad (7)$$

And the total deflection of the two teeth in contact thus takes the form

$$\delta_t = \delta_p + \delta_g = K \frac{w_r}{E} \left[\frac{h_p}{t_p} \cos \theta_p + \frac{h_g}{t_g} \cos \theta_g \right] \quad (8)$$

This empirical formula conforms quite closely to the results obtained from the deflection tests, and it can be used as a base to evaluate gear-tooth load distribution.

Since Walker's empirical formula of tooth deflection still has three variables h , t and θ involved, and in order to simplify it, assumptions are made as follows: (See Fig. 8)

- (1) Let thickness t equal to the arc length MN instead of chord length MN for small tooth thickness angle. Then $t = \overline{MN} \approx \widehat{MN}$

(2) If the fillet radius is small, the tangent points M and N of the constant stress parabola to the fillet radius have a negligibly slight change and assumed to be a constant, i.e.,

$$t \approx \widehat{MN} = \text{arc root thickness}$$

(3) The chordal height UV is small compared to the length h and can be neglected. Then $h \approx \overline{QU}$

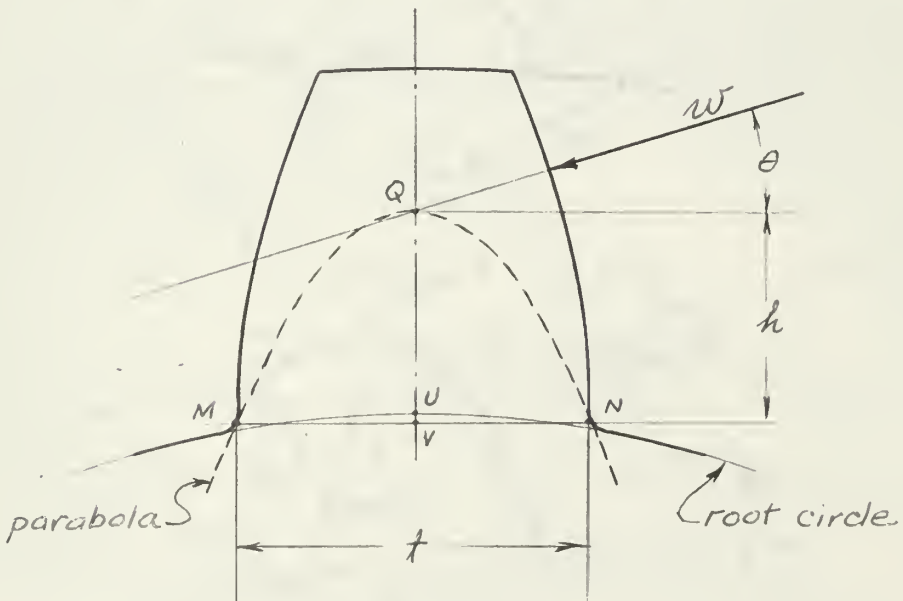


Fig. 8. Governing variables of tooth deflection

From these assumptions, the empirical formula of tooth deflection can be simplified for the two variables h and θ . Fig. 9 shows the relation of h and θ for both pinion and gear separately when two pairs of teeth are in contact. Taking the pitch point O as the reference point, when teeth are moved from the solid-line position to the dotted-line position, one of the contact points for first pair of teeth P and G , is α , and another

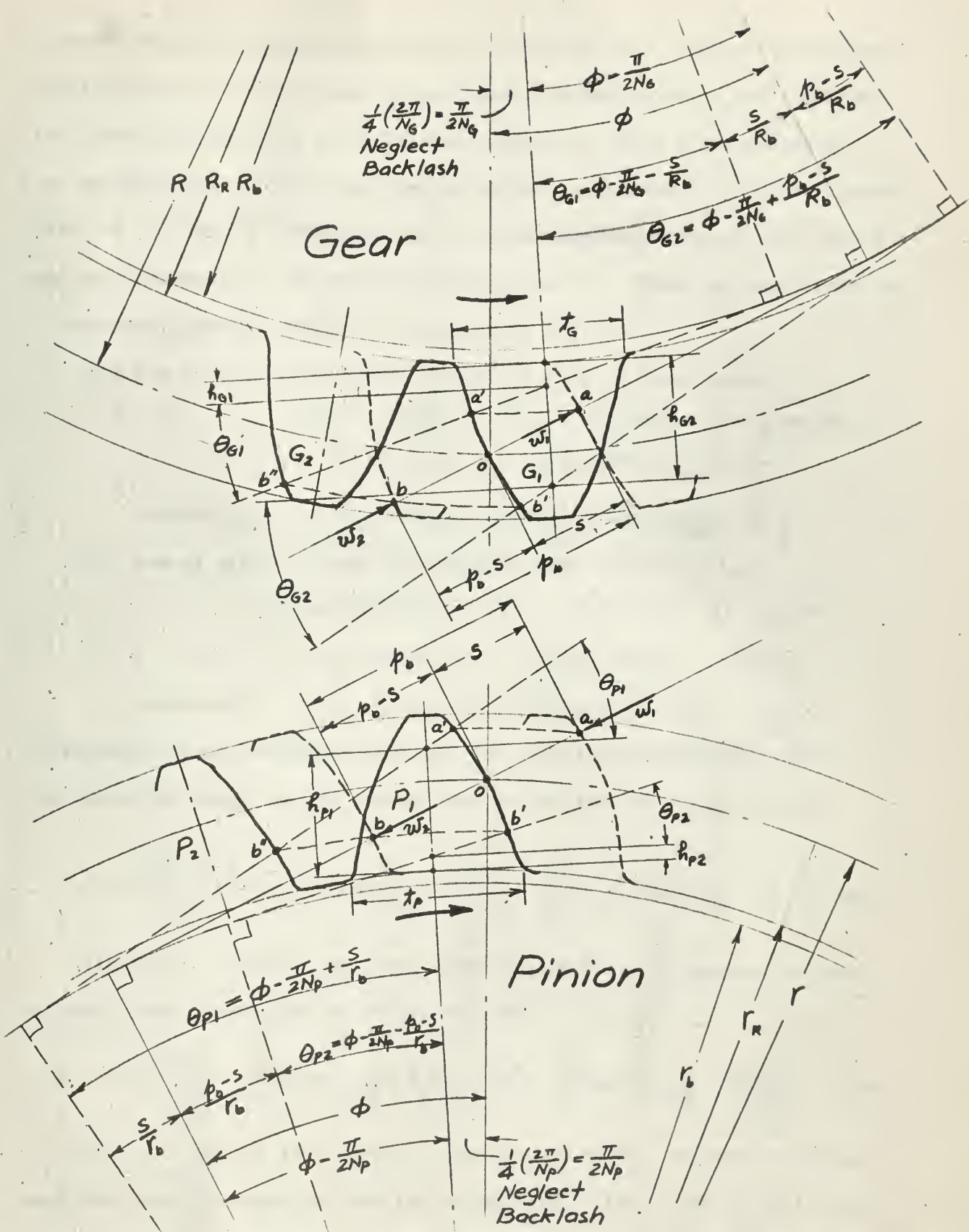


Fig. 19. Relation of load applied angle for both pinion and gear showing separately, when two pairs of teeth are in contact.

contact point for second pair of teeth P_2 and G_2 is b , the value of load applied angle θ can be found by the corresponding point on the teeth of the pinion and the gear at solid-line position. Then a' corresponds to a on the recess side of the line of action, a distance S from the pitch point o ; b' and b'' correspond to b on the approach side of the line of action, a distance $p_b - S$ from the pitch point o . Thus, by the properties of involute geometry, which is indicated in Fig. 9:

For the first pair of teeth (on recess side of pitch point)

$$h_{p_1} = \frac{r_b}{\cos \theta_{p_1}} - r_R; \quad h_{p_1} \cos \theta_{p_1} = r_b - r_R \cos \theta_{p_1}$$

$$\therefore h_{p_1} \cos \theta_{p_1} = r_b - r_R \cos \left(\phi - \frac{\pi}{2N_p} + \frac{S}{r_b} \right)$$

similarly $h_{G_1} \cos \theta_{G_1} = R_b - R_R \cos \left(\phi - \frac{\pi}{2N_G} - \frac{S}{R_b} \right)$

For second pair of teeth (on approach side of pitch point)

$$h_{p_2} = \frac{r_b}{\cos \theta_{p_2}} - r_R; \quad h_{p_2} \cos \theta_{p_2} = r_b - r_R \cos \theta_{p_2}$$

$$\therefore h_{p_2} \cos \theta_{p_2} = r_b - r_R \cos \left(\phi - \frac{\pi}{2N_p} - \frac{p_b - S}{r_b} \right)$$

similarly $h_{G_2} \cos \theta_{G_2} = R_b - R_R \cos \left(\phi - \frac{\pi}{2N_G} + \frac{p_b - S}{R_b} \right)$

Substituting these relations into Eq. (8), the total deflection of the two teeth in contact on the recess side of the line of action will be

$$\delta_r = K \frac{w_1}{E} \left\{ \left[\frac{r_b}{f_p} - \frac{r_R}{f_p} \cos \left(\phi - \frac{\pi}{2N_p} + \frac{S}{r_b} \right) \right] + \left[\frac{R_b}{f_G} - \frac{R_R}{f_G} \cos \left(\phi - \frac{\pi}{2N_G} - \frac{S}{R_b} \right) \right] \right\} \quad (9)$$

Similarly, the total deflection of the two teeth in contact on the approach side of the line of action will be

$$\delta_a = K \frac{w_2}{E} \left\{ \left[\frac{r_b}{f_p} - \frac{r_R}{f_p} \cos \left(\phi - \frac{\pi}{2N_p} + \frac{S - p_b}{r_b} \right) \right] + \left[\frac{R_b}{f_G} - \frac{R_R}{f_G} \cos \left(\phi - \frac{\pi}{2N_G} - \frac{S - p_b}{R_b} \right) \right] \right\} \quad (10)$$

The Eqs. (9) and (10) involve a variable S only. In order to determine the load distribution from the deflection of the teeth, we will make use of the fact that the sum of the deflections of the pair of teeth on

the recess side must be equal to the sum of the deflections of the pair of teeth on the approach side, or we can use the combined stiffness to determine the load distribution at each side.

The term of combined stiffness is defined as the load required to produce unit total deflections. Let it be denoted by λ , then

$$\lambda_r = \bar{w}_1 \quad \text{when} \quad \delta_r = 1$$

$$\lambda_a = \bar{w}_2 \quad \text{when} \quad \delta_a = 1$$

therefore

$$\lambda_r = \frac{E/K}{\left[\frac{r_b}{\bar{f}_p} - \frac{r_b}{\bar{f}_p} \cos(\phi - \frac{\pi}{2N_p} + \frac{s}{r_b}) \right] + \left[\frac{r_b}{\bar{f}_g} - \frac{r_b}{\bar{f}_g} \cos(\phi - \frac{\pi}{2N_g} - \frac{s}{r_b}) \right]} \quad (11)$$

$$\lambda_a = \frac{E/K}{\left[\frac{r_b}{\bar{f}_p} - \frac{r_b}{\bar{f}_p} \cos(\phi - \frac{\pi}{2N_p} + \frac{s - p_b}{r_b}) \right] + \left[\frac{r_b}{\bar{f}_g} - \frac{r_b}{\bar{f}_g} \cos(\phi - \frac{\pi}{2N_g} - \frac{s - p_b}{r_b}) \right]} \quad (12)$$

and the load distribution can be expressed as

$$\text{At approach side: } \bar{w}_a = \frac{\lambda_a}{\lambda_a + \lambda_r} \cdot W \quad (13)$$

$$\text{At recess side: } \bar{w}_r = \frac{\lambda_r}{\lambda_a + \lambda_r} \cdot W \quad (14)$$

where \bar{w}_a = load carried by a pair of teeth on approach side of line of action when two pairs of teeth are in contact.

\bar{w}_r = load carried by a pair of teeth on recess side of line of action when two pairs of teeth are in contact.

W = total transmitted load normal to tooth surface.

If the same kind of material is used for both the pinion and the gear, the factor E/K will be cancelled when Eqs. (11) and (12) are substituted into Eqs. (13) and (14), which will then be a function of s only.

The root thickness \bar{f}_p and \bar{f}_g in Eqs. (11) and (12) depend upon whether the root circle diameter is greater or smaller than the base circle diameter. In Fig. 9, the root circle diameter is drawn greater than the base circle diameter. Sometimes the root circle diameter is smaller than the

base circle diameter, depending on the number of teeth. For standard full-depth tooth:

$$\text{root circle diameter } d_r = d - 2 \frac{1.157}{P_d} = d \left(1 - \frac{2.314}{N}\right)$$

$$\text{base circle diameter } d_b = d \cos \phi$$

$$\therefore \frac{d_r}{d_b} = \frac{1 - \frac{2.314}{N}}{\cos \phi}$$

when $\phi = 14\frac{1}{2}^\circ$ if $d_r > d_b$,

$$1 - \frac{2.314}{N} > \cos 14\frac{1}{2}^\circ \quad \therefore N \geq 73$$

when $\phi = 20^\circ$ if $d_r > d_b$,

$$1 - \frac{2.314}{N} > \cos 20^\circ \quad \therefore N \geq 39$$

when $\phi = 25^\circ$ if $d_r > d_b$

$$1 - \frac{2.314}{N} > \cos 25^\circ \quad \therefore N \geq 25$$

For 20° stub tooth: $d_r = d - 2 \cdot \frac{1}{P_d} = d \left(1 - \frac{2}{N}\right)$

if $d_r > d_b$

$$1 - \frac{2}{N} > \cos 20^\circ \quad \therefore N \geq 34$$

In case of $d_r > d_b$, referring to Fig. 10,

$$t = 2r_R \left[\frac{\pi}{2N_p} + (\text{Inv} \phi - \text{Inv} \delta_p^*) \right]$$

where

$$\text{Inv} \phi = \frac{r_b \tan \phi}{r_b} - \phi = \frac{\sqrt{r^2 - r_b^2}}{r_b} - \tan^{-1} \frac{\sqrt{r^2 - r_b^2}}{r_b}$$

$$\text{Inv} \delta^* = \frac{r_b \tan \delta^*}{r_b} - \delta^* = \frac{\sqrt{r_R^2 - r_b^2}}{r_b} - \tan^{-1} \frac{\sqrt{r_R^2 - r_b^2}}{r_b}$$

For pinion:

$$t_p = d_R \left[\frac{\pi}{2N_p} + (\text{Inv} \phi - \text{Inv} \delta_p^*) \right] \quad (15)$$

For gear:

$$t_g = D_R \left[\frac{\pi}{2N_g} + (\text{Inv} \phi - \text{Inv} \delta_g^*) \right] \quad (16)$$

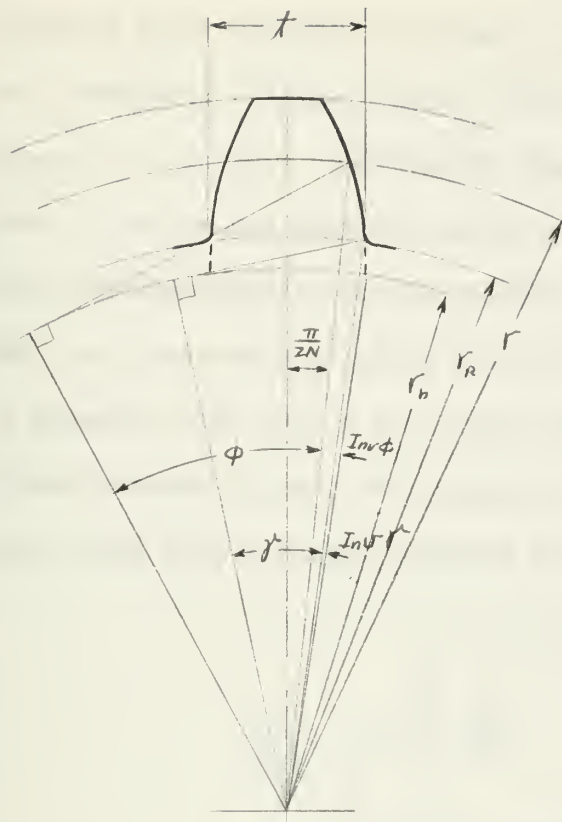


Fig. 10 Root thickness when $d_r > d_b$

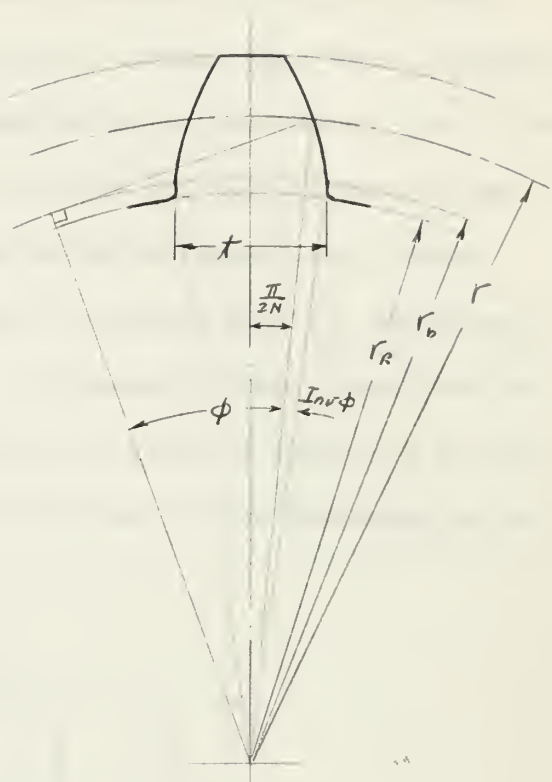


Fig. 11 Root thickness when $d_r < d_b$

In case $d_r < d_b$, referring to Fig. 11, where $\gamma = 0$

For pinion:

$$t_p = d_r \left[\frac{\pi}{2N_p} + \text{Inv} \phi \right] \quad (17)$$

For gear:

$$t_g = D_r \left[\frac{\pi}{2N_g} + \text{Inv} \phi \right] \quad (18)$$

We now return to the load distribution Eqs. (13) and (14). The variable S is included in the argument of the cosine function, occurring in both the numerator and denominator. The behavior of these functions can not be seen directly. We are interested in how they behave on the approach and the recess sides when two pairs of teeth are in contact.

Various numbers of teeth, 20, 40, 80, 100, 200 and 400, all of 20° pressure angle standard full-depth, and unit diametral pitch, are chosen for systematic calculations at various velocity ratios (gear ratio) combinations. The results, showing the load distribution on the recess side of the line of action are plotted in Fig. 13, 14, 15 and 16. It is obvious that the load distribution on the approach side would be symmetrically equal. The load distribution curves are now shaped as seen in Fig. 12, which may be compared with Fig. 6 for rigid teeth. Fortunately, these curves are inclined straight lines, which means that when two pairs of teeth are in contact, they take a lesser fraction of the total load at the beginning and at

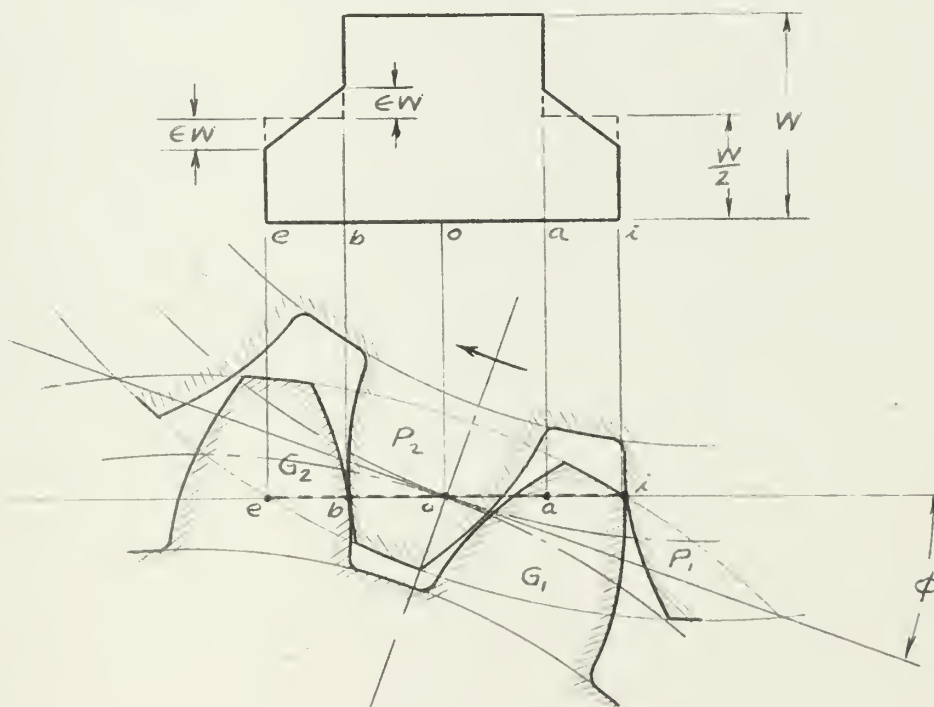


Fig. 12. Load distribution of elastic teeth.

the end of contact and increase gradually to a greater fraction of the total load as they approach and depart from the region in which a single pair of teeth take the load. Where ϵ depends on the number of teeth in combination.

Sample calculation for a 40 tooth pinion and an 80 tooth gear is given in the Appendix I.

The nature of the tooth load distribution evaluated based on these assumptions are shown in Fig. 13, 14, 15 and 16. They cover all of the practical cases. From the curves we see that the straight line equation can be used to express these load distributions.

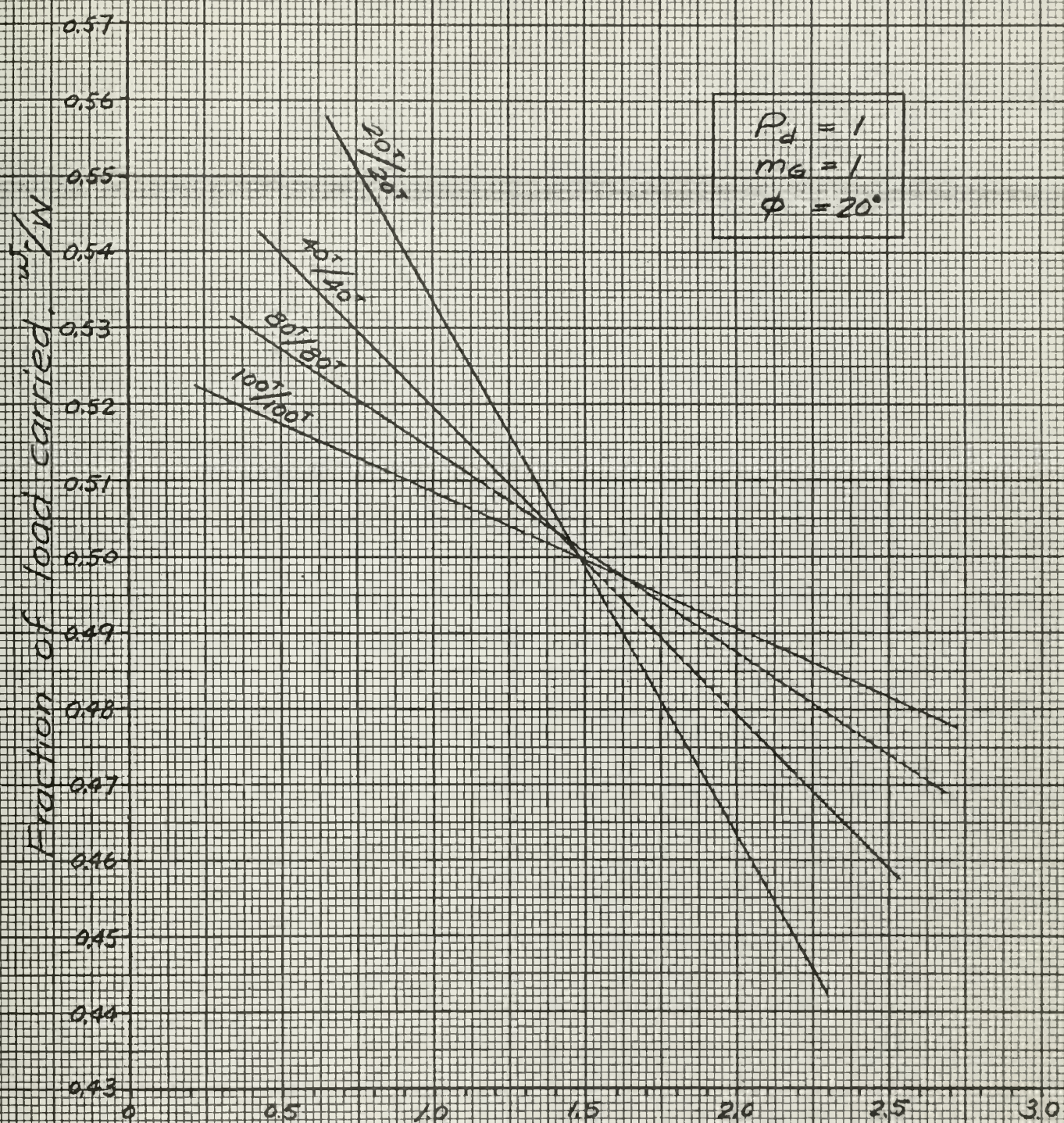


FIG. 13. Load distribution on the recess side of line of action of 20° full-depth teeth.

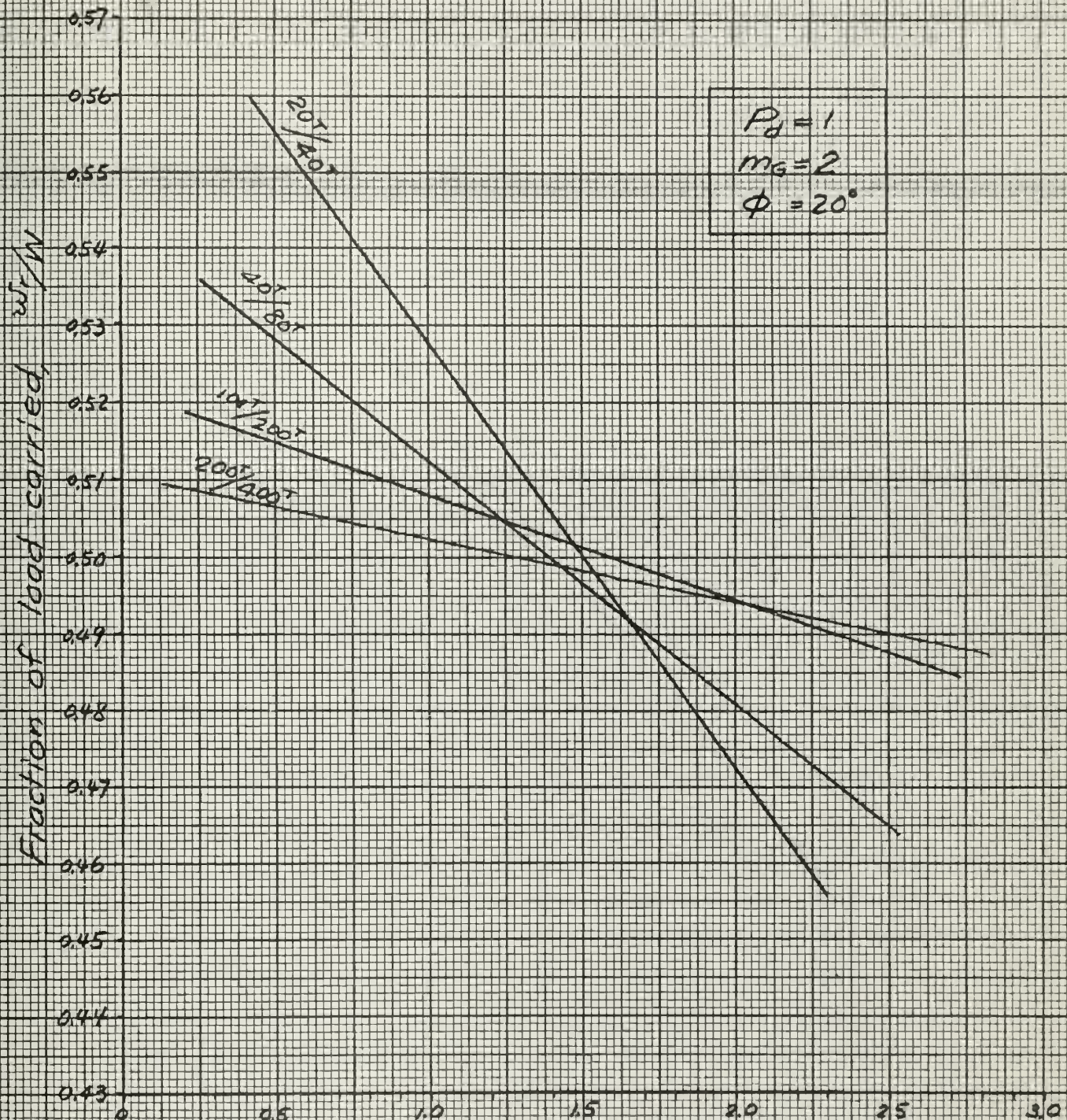


Fig. 14. Load distribution on the recess side of line of action of 20° full-depth teeth.

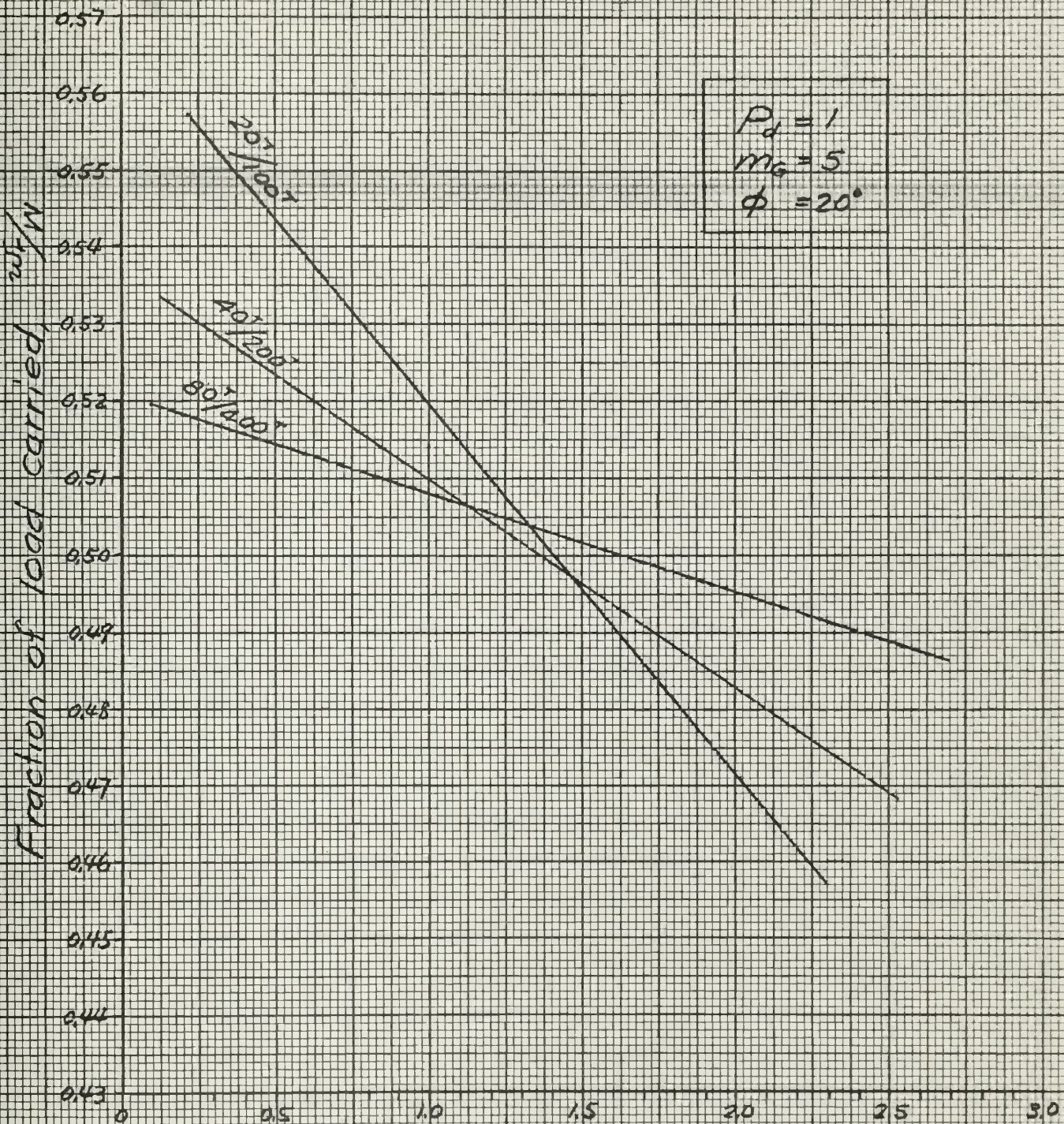
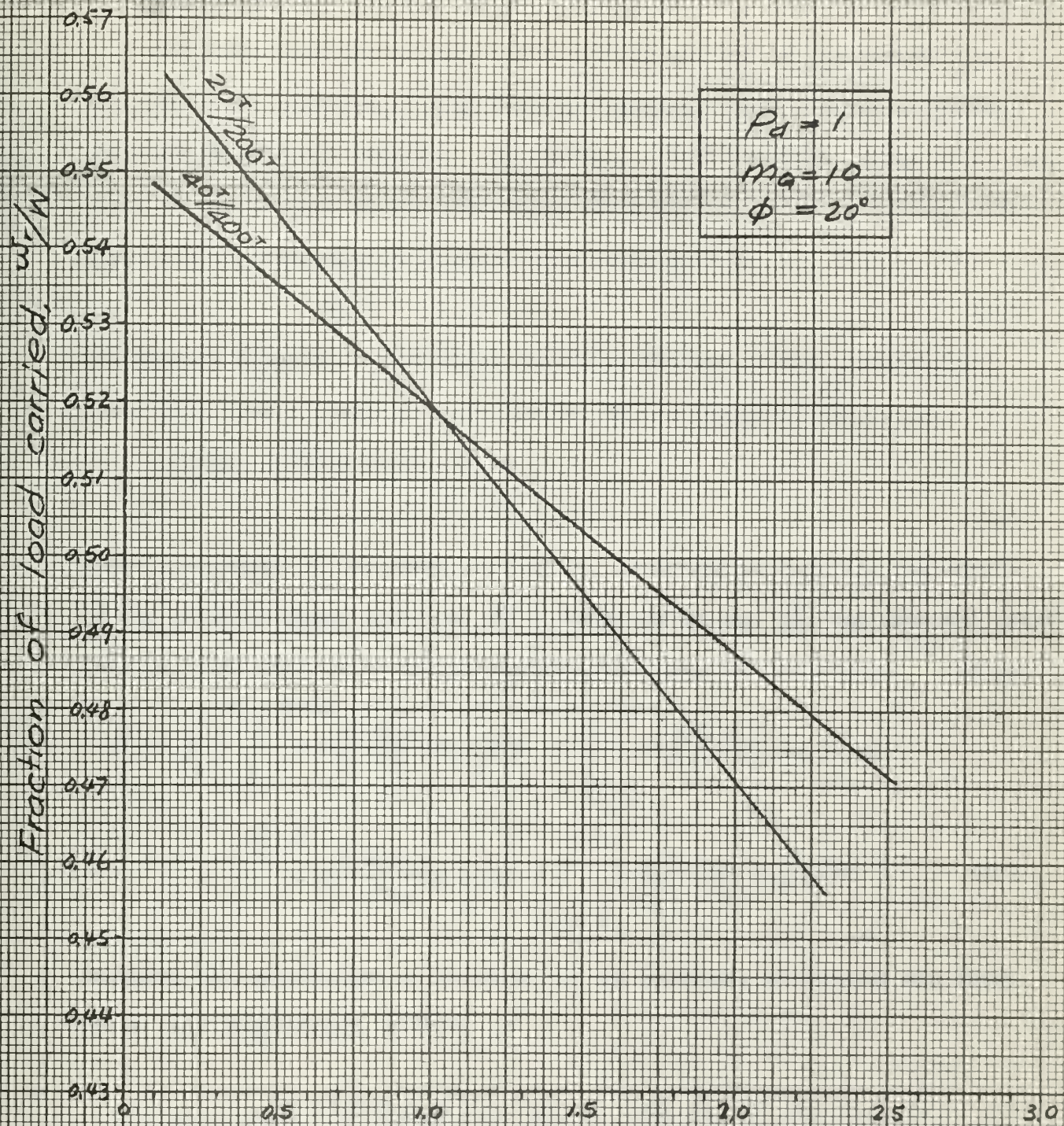


Fig. 15. Load distribution on the recess side of line of action of 20° full-depth teeth.



Distance from pitch point to point of contact at recess side, s [in]

Fig. 16. Load distribution on the recess side of line of action of 20° full-depth teeth.

V. Power Loss

The power loss due to gear tooth sliding now can be calculated with the aid of the relative sliding velocity and gear tooth load distribution obtained in previous articles. By the basic considerations, since frictional power is the product of the frictional force and the relative sliding velocity, the instantaneous frictional power loss will be

$$P_f = \mu \cdot w \cdot v \quad (19)$$

The average frictional power loss should be the sum of the instantaneous power loss over a complete cycle divided by the length of the cycle.

In case of rigid teeth, it is

$$P_f = \frac{1}{L} \int \mu w v ds \quad (20)$$

where L = length of the power loss cycle, referring to Fig. 17, the length of the friction power cycle is P_b . Substituting Eq. (2) for external gears into Eq. (20) and for a contact ratio in the range of $1 < m_p < 2$, we get

$$P_f = \frac{1}{P_b} \left\{ \int_0^{P_b - Z_r} \mu w \left[\left(\frac{m_g + 1}{m_g} \right) \omega_p s \right] ds + \int_{P_b - Z_r}^{Z_a} \mu \frac{w}{2} \left[\left(\frac{m_g + 1}{m_g} \right) \omega_p s \right] ds \right. \\ \left. + \int_0^{P_b - Z_a} \mu w \left[\left(\frac{m_g + 1}{m_g} \right) \omega_p s \right] ds + \int_{P_b - Z_a}^{Z_r} \mu \frac{w}{2} \left[\left(\frac{m_g + 1}{m_g} \right) \omega_p s \right] ds \right\} \quad (21)$$

Assuming the coefficient of friction μ is constant, performing the integrals, and simplifying, we have

$$P_f = \mu \frac{w \omega_p (m_g + 1)}{2} \left[\frac{Z_a^2 + Z_r^2}{2 P_b} + \frac{(P_b - Z_a)^2 + (P_b - Z_r)^2}{2 P_b} \right] \quad (22)$$

The power loss diagram shown in Fig. 17 occurs in most cases in standard interchangeable gear systems, but for the $14 \frac{1}{2}^\circ$ full-depth tooth in the region of $1 < m_p < 2$, some gear combinations have $Z_a > P_b$.

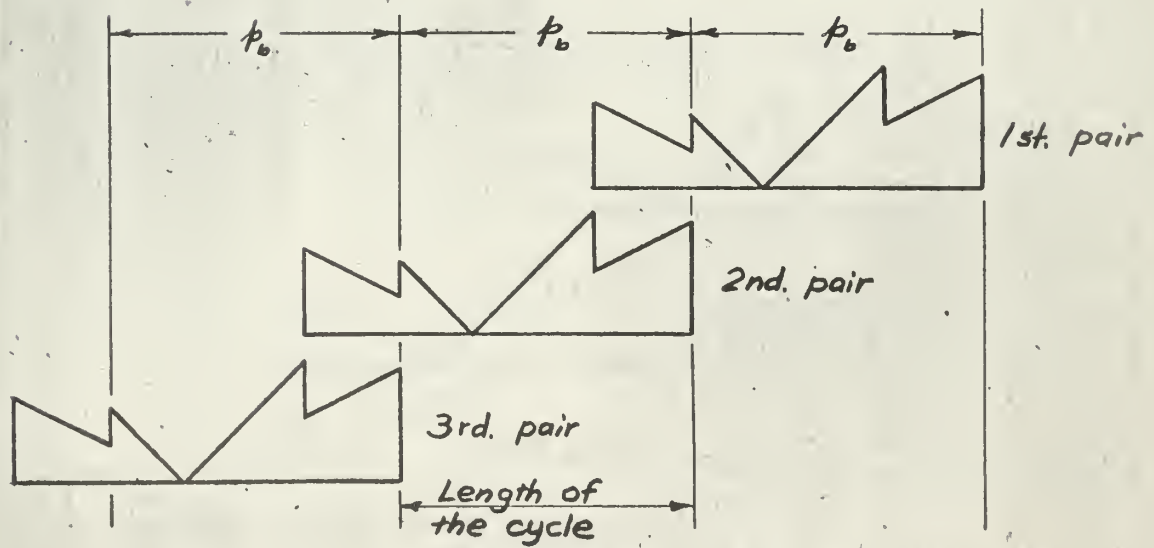
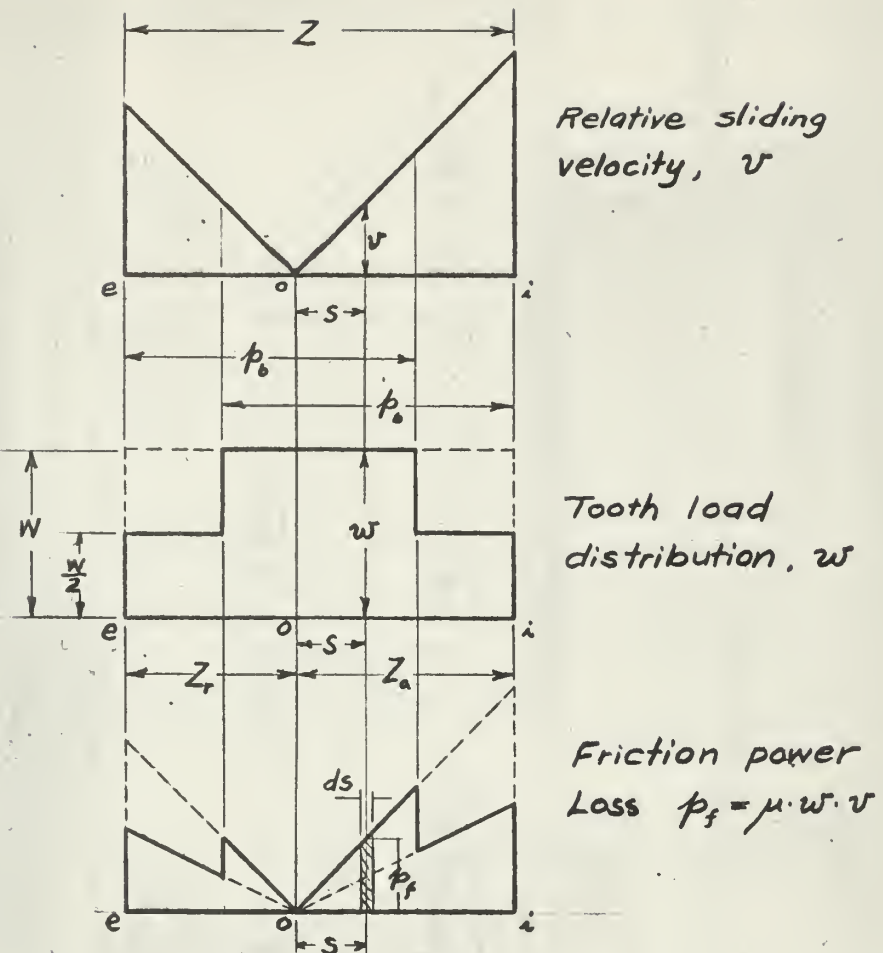
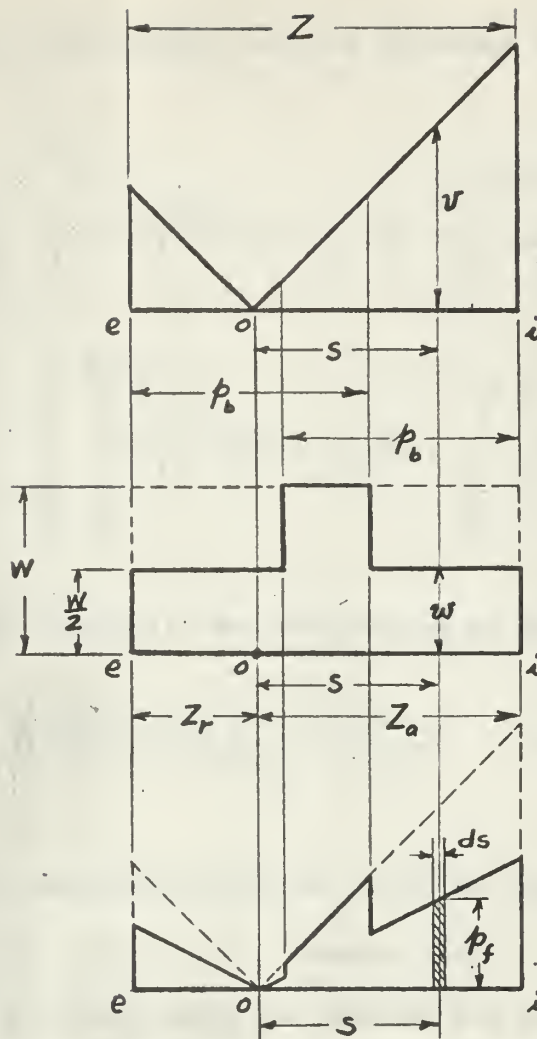


Fig. 17. Power loss diagram and cycles for rigid tooth when $1 < m_p < 2$; $p_0 > Z_a$; $p_0 > Z_r$



Relative sliding velocity, v

Tooth load distribution, w

Friction power loss $p_f = \mu \cdot w \cdot v$

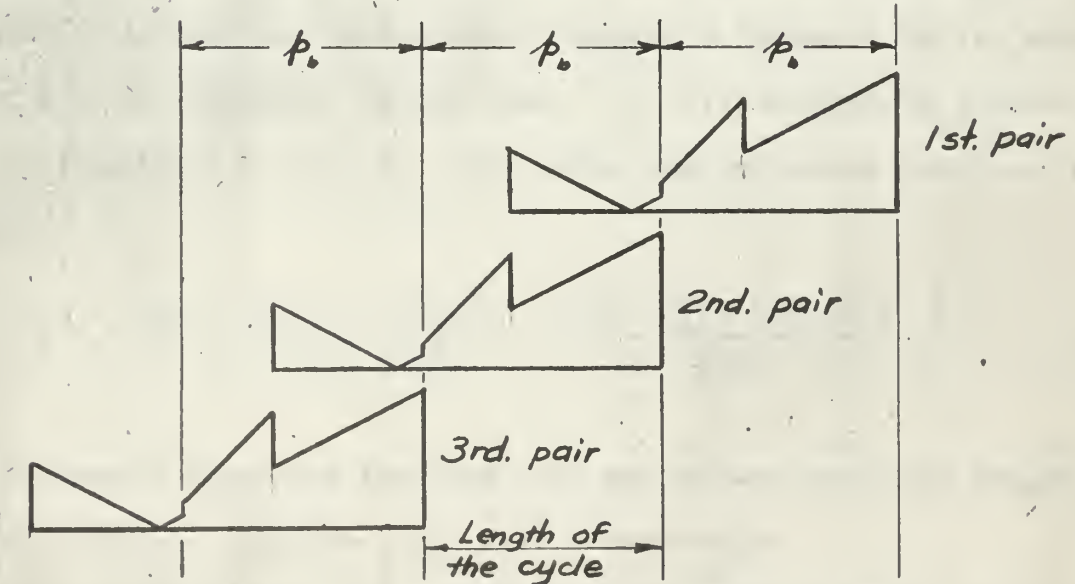


Fig. 17a. Power loss diagram and cycles for rigid tooth when $1 < m_p < 2$; $p_b < Z_a$; $p_b > Z_r$

then the power loss diagram will be different in shape as shown in Fig.

17a, and

$$P_f = \frac{1}{p_b} \left\{ \int_0^{Z_r} \mu \frac{W}{2} \left[\left(\frac{m_g+1}{m_g} \right) \omega_p s \right] ds + \int_{Z_a - p_b}^{Z_a} \mu \frac{W}{2} \left[\left(\frac{m_g+1}{m_g} \right) \omega_p s \right] ds \right. \\ \left. + \int_{Z_a - p_b}^{p_b - Z_r} \mu W \left[\left(\frac{m_g+1}{m_g} \right) \omega_p s \right] ds + \int_{p_b - Z_r}^{Z_a} \mu \frac{W}{2} \left[\left(\frac{m_g+1}{m_g} \right) \omega_p s \right] ds \right\}$$

performing the integrals, and simplifying we have

$$P_f = \mu \frac{W \omega_p}{2} \left(\frac{m_g+1}{m_g} \right) \left[\frac{Z_a^2 + Z_r^2}{2 p_b} + \frac{-(p_b - Z_a)^2 + (p_b - Z_r)^2}{2 p_b} \right] \quad (22a)$$

Comparing this expression with Eq. (22), we find each term will be the same in magnitude but $(p_b - Z_a)^2$ changes sign.

In some practical gears the addenda are modified for other design requirements, in general, the addendum of pinion is increased and the addendum of gear is decreased. In this case, Z_r will possibly be greater than p_b . Similarly, if $Z_r > p_b$, the power loss expression will be in the form of

$$P_f = \mu \frac{W \omega_p}{2} \left(\frac{m_g+1}{m_g} \right) \left[\frac{Z_a^2 + Z_r^2}{2 p_b} + \frac{(p_b - Z_a)^2 - (p_b - Z_r)^2}{2 p_b} \right] \quad (22b)$$

This expression also shows that each term has the same magnitude compared with Eq. (22), but the term $(p_b - Z_r)^2$ changes sign.

If we substitute Eq. (3) into Eq. (20) for internal gears, then the form of Eq. (22) will change only the factor from $\left(\frac{m_g+1}{m_g} \right)$ to $\left(\frac{m_g-1}{m_g} \right)$.

In the case of elastic teeth, before performing any integrations to determine the average frictional power loss, it is necessary to establish a straight line equation for the tooth load distribution in a form which will be simpler than that of Eqs. (13) and (14), and also satisfy the nature of load distribution as shown in Fig. 13, 14, 15 and 16. Referring to Fig. 18, on the approach side of line of action,

$$W_a = \frac{W}{2} + \epsilon W \quad \text{when} \quad S = p_b - Z_r$$

$$W_a = \frac{W}{2} - \epsilon W \quad \text{when} \quad S = Z_a$$

Then the straight line equation will be

$$W_a = \frac{W}{2} + \left[\epsilon W \frac{-p_b - Z_a + Z_r}{p_b - Z_a - Z_r} + 2\epsilon W \frac{S}{p_b - Z_a - Z_r} \right] \quad (23)$$

Similarly, the load on the recess side is

$$W_r = \frac{W}{2} + \left[\epsilon W \frac{-p_b + Z_a - Z_r}{p_b - Z_a - Z_r} + 2\epsilon W \frac{S}{p_b - Z_a - Z_r} \right] \quad (24)$$

Denote the second terms in Eq. (23) and (24) by w_a' and w_r' respectively, and the relative sliding velocity by Eq. (2); then the average frictional power loss for external gears and $1 < m_p < 2$. Eq. (20) can be written

$$P_f = \frac{1}{p_b} \left\{ \int_0^{p_b - Z_r} \mu W \left[\left(\frac{m_p + 1}{m_p} \right) \omega_p s \right] ds + \int_0^{p_b - Z_a} \mu W \left[\left(\frac{m_p + 1}{m_p} \right) \omega_p s \right] ds \right. \\ + \int_{p_b - Z_r}^{Z_a} \mu \frac{W}{2} \left[\left(\frac{m_p + 1}{m_p} \right) \omega_p s \right] ds + \int_{p_b - Z_a}^{Z_r} \mu \frac{W}{2} \left[\left(\frac{m_p + 1}{m_p} \right) \omega_p s \right] ds \\ \left. + \int_{p_b - Z_r}^{Z_a} \mu w_a' \left[\left(\frac{m_p + 1}{m_p} \right) \omega_p s \right] ds + \int_{p_b - Z_a}^{Z_r} \mu w_r' \left[\left(\frac{m_p + 1}{m_p} \right) \omega_p s \right] ds \right\} \quad (25)$$

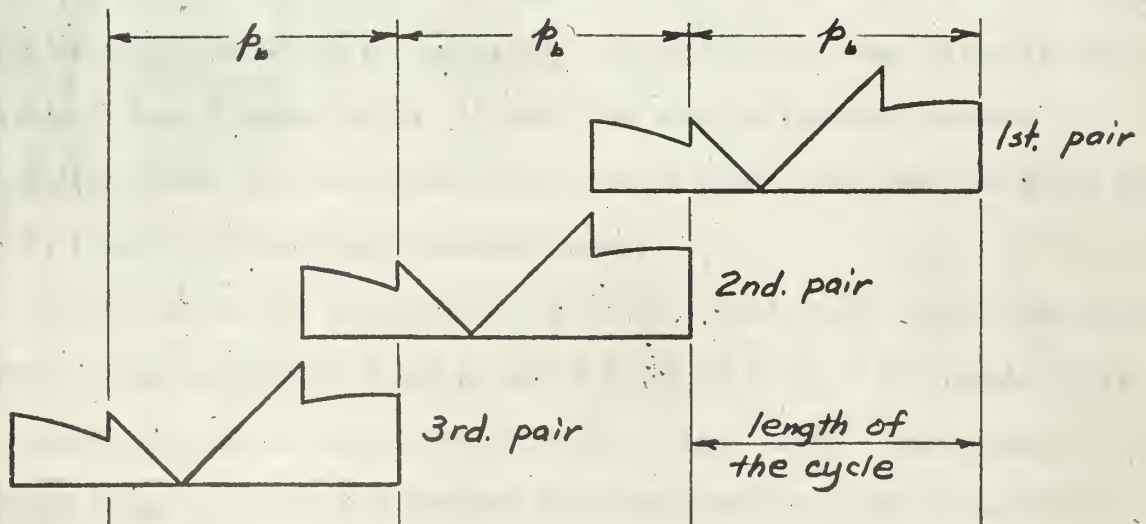
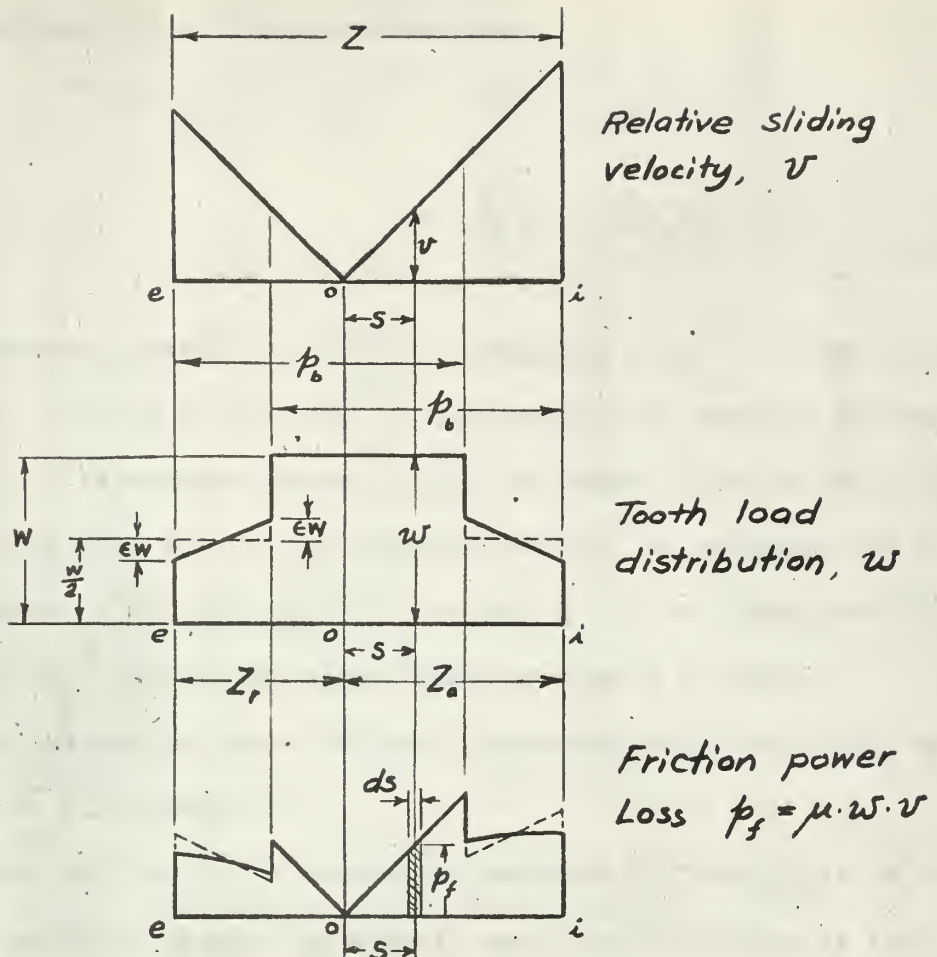


Fig. 18. Power loss diagram and cycles for elastic tooth when $1 < m_p < 2$; $p_b > Z_a$; $p_b > Z_r$.

The integration of this equation gives

$$P_f = \mu \frac{W\omega_p}{2} \left(\frac{m_g + 1}{m_g} \right) \left[\frac{Z_a^2 + Z_r^2}{2p_n} + \frac{(p_n - Z_a)^2 + (p_n - Z_r)^2}{2p_n} - \epsilon \frac{2}{3p_n} (Z_a + Z_r - p_n)^2 \right] \quad (26)$$

For internal gears, use $\left(\frac{m_g - 1}{m_g} \right)$ instead of $\left(\frac{m_g + 1}{m_g} \right)$. The brackets of Eq. (26), contain a term with ϵ in addition to those in the brackets in Eq. (22). If various numbers of 20° full-depth standard teeth are chosen, as has been done in the previous article, to calculate the terms in the bracket of Eq. (22) and (26), values of ϵ are taken from Fig. 13, 14, 15, and 16. Results and comparisons are listed in Table I.

Sample calculation for a 40 tooth pinion and an 80 tooth gear combination is given in Appendix II.

From the results of the comparison obtained in Table I, it is seen that the frictional power loss of an elastic tooth due to sliding is less than that of a rigid gear tooth, and the percentage of differences based on rigid tooth is small enough to be neglected. It can also be seen directly from the power-loss diagram in Fig. 18 that the area differences between the solid-line curve and the dotted-line curve is small, and that the total areas can be treated as being approximately equal.

By the use of the approximation that is stated above in the case where contact ratio is between 2 and 3, which occur in $14 \frac{1}{2}^\circ$ full-depth teeth, we proceed with these calculations based on rigid teeth. Referring to Fig. 19, for external gears, the average friction power loss can be expressed approximately as

TABLE 1.

Comparison of friction loss of rigid teeth and elastic teeth:

Gear ratio	$\frac{N_p}{N_g}$	** Rigid Tooth friction loss	* Additional Elastic tooth friction loss	Percentage of diff. based on rigid tooth
1	20T/20T	0.655	-0.0114	-1.74
	40T/40T	0.755	-0.0145	-1.92
	80T/80T	0.839	-0.0136	-1.62
	100T/100T	0.860	-0.0137	-1.59
2	20T/40T	0.705	-0.0163	-2.31
	40T/80T	0.799	-0.0144	-1.80
	100T/200T	0.896	-0.0097	-1.09
	200T/400T	0.931	-0.0058	-0.62
5	20T/100T	0.760	-0.0192	-2.53
	40T/200T	0.835	-0.0150	-1.80
	80T/400T	0.893	-0.0105	-1.17
10	20T/200T	0.786	-0.0217	-2.75
	40T/400T	0.850	-0.0220	-2.60

** Calculated from the bracket of Eq. (22) divided by ρ_b .* Calculated from the bracket of additional term of Eq. (26) containing ϵ divided by ρ_b .

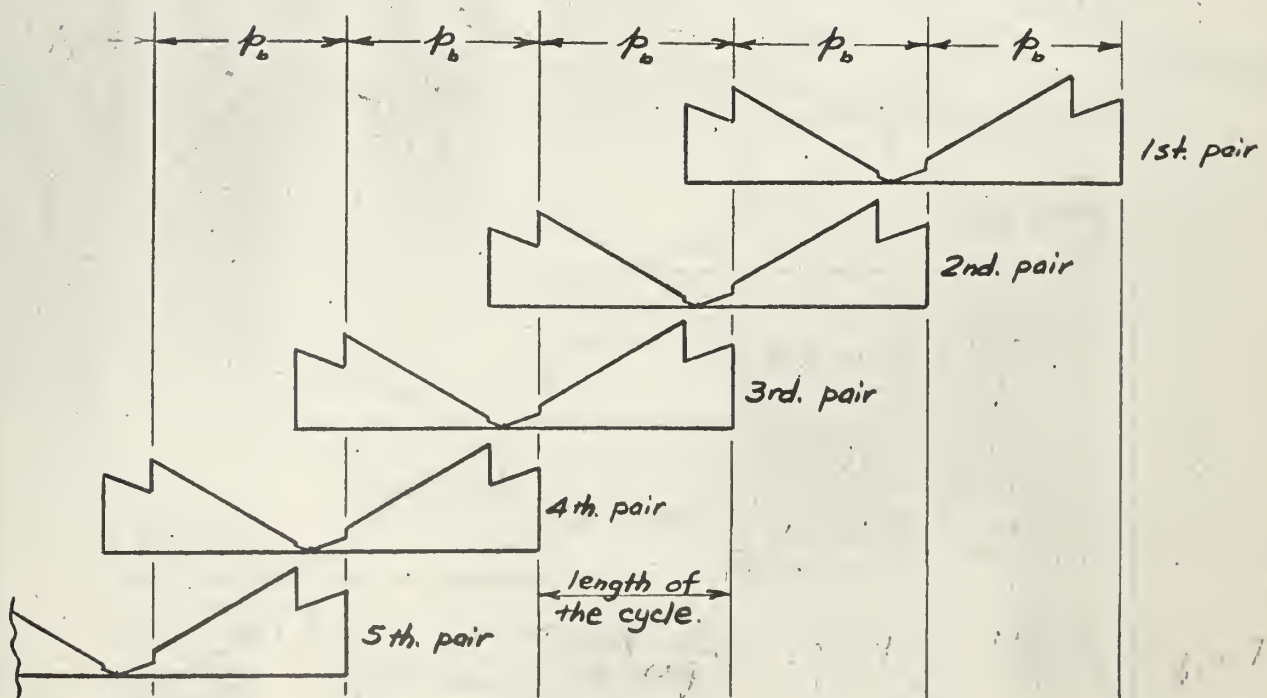
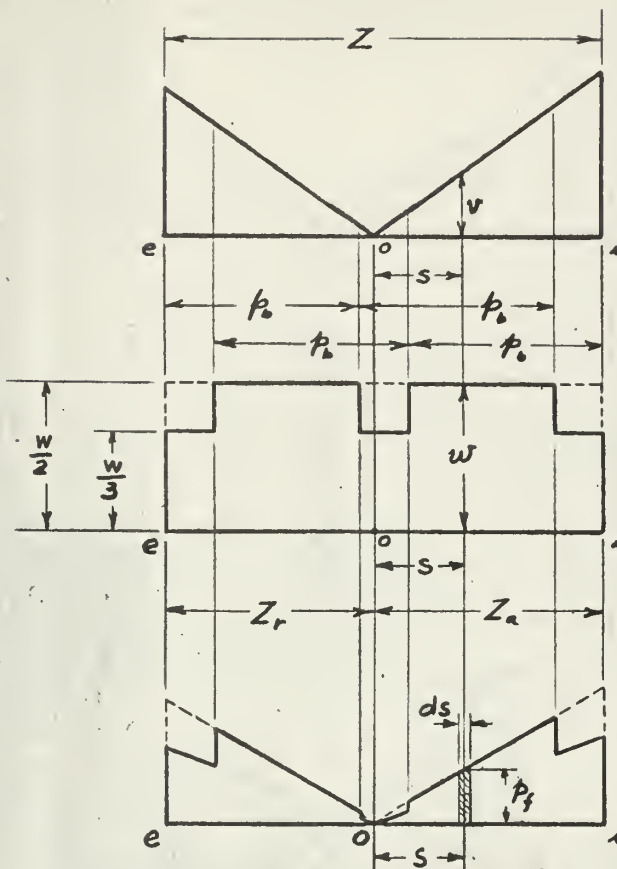


Fig. 19. Power loss diagram and cycles for rigid tooth when $2 < m_p < 3$; $Z_a > p_0$; $Z_r > p_0$

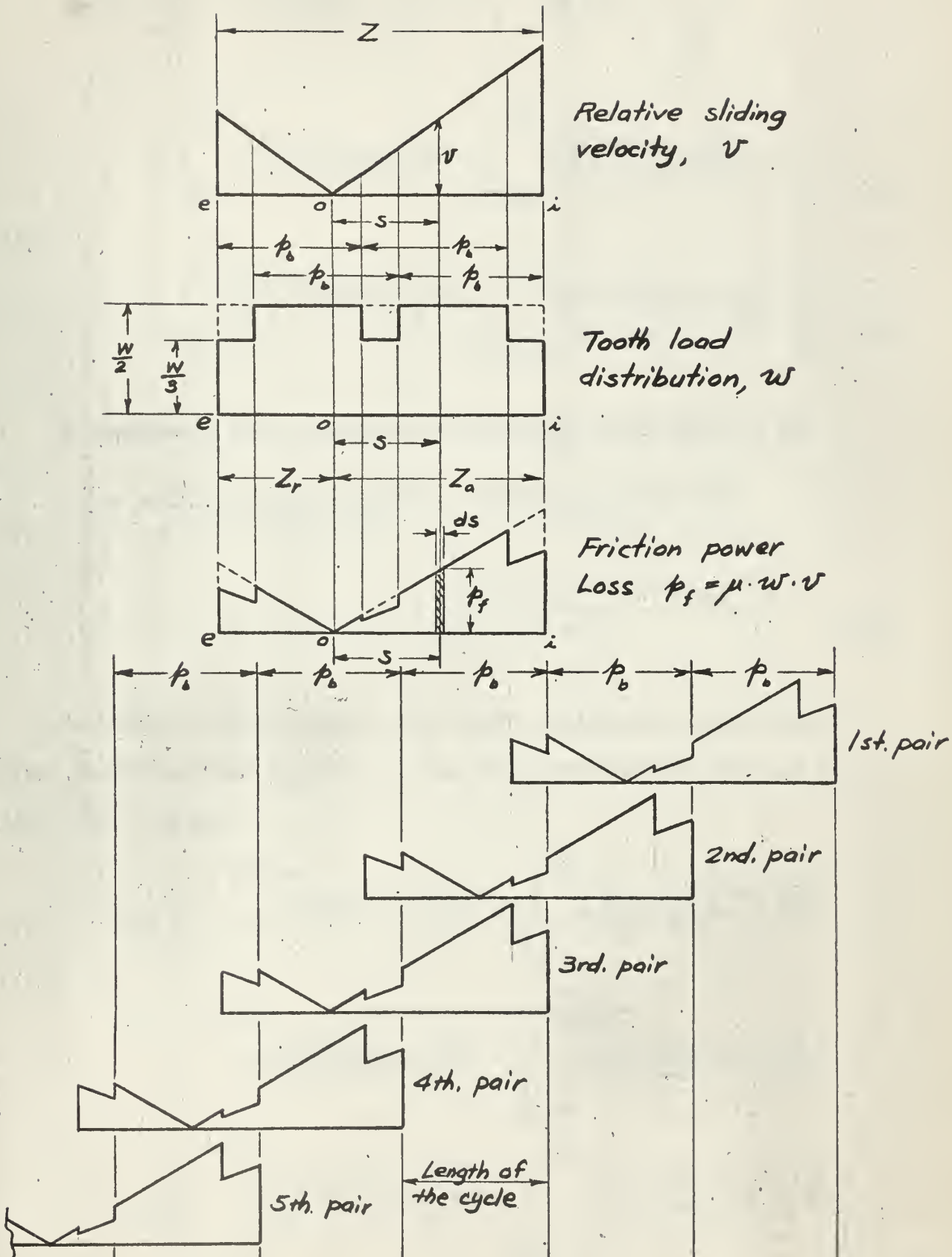


Fig. 19a. Power loss diagram and cycles for rigid tooth when $2 < m_p < 3$; $Z_a > p_o$; $Z_r < p_o$

$$\begin{aligned}
P_f = \frac{1}{p_b} \left\{ \int_0^{Z_a - p_b} \mu \frac{w}{3} \left[\left(\frac{m_g+1}{m_g} \right) \omega_p s \right] ds + \int_0^{Z_r - p_b} \mu \frac{w}{3} \left[\left(\frac{m_g+1}{m_g} \right) \omega_p s \right] ds \right. \\
+ \int_{Z_a - p_b}^{2p_b - Z_a} \mu \frac{w}{2} \left[\left(\frac{m_g+1}{m_g} \right) \omega_p s \right] ds + \int_{Z_r - p_b}^{2p_b - Z_a} \mu \frac{w}{2} \left[\left(\frac{m_g+1}{m_g} \right) \omega_p s \right] ds \\
\left. + \int_{2p_b - Z_a}^{Z_a} \mu \frac{w}{3} \left[\left(\frac{m_g+1}{m_g} \right) \omega_p s \right] ds + \int_{2p_b - Z_a}^{Z_r} \mu \frac{w}{3} \left[\left(\frac{m_g+1}{m_g} \right) \omega_p s \right] ds \right\} \quad (27)
\end{aligned}$$

By performing the integrations, the average power loss will be

$$\begin{aligned}
P_f = \mu \frac{w \omega_p}{2} \left(\frac{m_g+1}{m_g} \right) \left[\frac{Z_a^2 + Z_r^2}{3p_b} + \frac{(2p_b - Z_a)^2 + (2p_b - Z_r)^2}{6p_b} \right. \\
\left. - \frac{(Z_a - p_b)^2 + (Z_r - p_b)^2}{6p_b} \right] \quad (28)
\end{aligned}$$

As before, in some cases of gear tooth combinations, p_b can sometimes be greater than Z_a or Z_r . Fig. 19a shows that for the case of $p_b > Z_r$, we have

$$\begin{aligned}
P_f = \frac{1}{p_b} \left\{ \int_0^{Z_r - p_b} \mu \frac{w}{2} \left[\left(\frac{m_g+1}{m_g} \right) \omega_p s \right] ds + \int_{Z_r - p_b}^{Z_r} \mu \frac{w}{3} \left[\left(\frac{m_g+1}{m_g} \right) \omega_p s \right] ds \right. \\
+ \int_0^{p_b - Z_r} \mu \frac{w}{2} \left[\left(\frac{m_g+1}{m_g} \right) \omega_p s \right] ds + \int_{p_b - Z_r}^{Z_a - p_b} \mu \frac{w}{3} \left[\left(\frac{m_g+1}{m_g} \right) \omega_p s \right] ds \\
\left. + \int_{Z_a - p_b}^{2p_b - Z_r} \mu \frac{w}{2} \left[\left(\frac{m_g+1}{m_g} \right) \omega_p s \right] ds + \int_{2p_b - Z_r}^{Z_a} \mu \frac{w}{3} \left[\left(\frac{m_g+1}{m_g} \right) \omega_p s \right] ds \right\}
\end{aligned}$$

Performing the integrals, and simplifying we have

$$P_f = \mu \frac{W\omega_p}{2} \left(\frac{m_g + 1}{m_g} \right) \left[\frac{Z_a^2 + Z_r^2}{3p_b} + \frac{(2p_b - Z_a)^2 + (2p_b - Z_r)^2}{6p_b} - \frac{(Z_a - p_b)^2 - (Z_r - p_b)^2}{6p_b} \right] \quad (28a)$$

Comparing this expression with Eq. (28), we find each term will be the same in magnitude but the term $(Z_r - p_b)^2$ changes sign. Similarly, if $p_b > Z_a$, the term $(Z_a - p_b)^2$ changes sign.

In case of the contact ratio m_p happens to be an integer, i.e., $p_b = Z_a + Z_r$ in Eq. (22) and $2p_b = Z_a + Z_r$ in Eq. (28), both Eq. (22) and (28) (taken $p_b > Z_a$ or $p_b > Z_r$ into account) will be reduced to the form

$$P_f = \mu \frac{W\omega_p}{2} \left(\frac{m_g + 1}{m_g} \right) \left[\frac{Z_a^2 + Z_r^2}{Z_a + Z_r} \right] \quad (29)$$

Eq. (29) is the particular case, which coincides with the results developed by Merritt [1] based on the assumption that the load distribution is constant across the entire line of action.

Therefore, in all practical standard or addendum modified teeth, the friction power loss due to gear tooth surface sliding can be calculated approximately and summarized as follows:

Case 1. When contact ratio is $1 < m_p < 2$

use Eq. (22). But if $Z_a > p_b$ or $Z_r > p_b$, the terms $(p_b - Z_a)^2$ or $(p_b - Z_r)^2$ should change sign respectively. (See Eq. 22a and 22b).

Case 2. When contact ratio is $2 < m_p < 3$ use Eq. (28). But if $p_b > Z_a$ or $p_b > Z_r$, the terms $(Z_a - p_b)^2$ or $(Z_r - p_b)^2$ should change sign respectively. (See Eq. 28a).

Case 3. When contact ratio is an integer, i.e., $m_p = 1$ or 2

use Eq. (29). In this case, no change of sign is necessary, because the load distribution becomes constant across entire line of action.

In all three cases, use $\left(\frac{m_G - 1}{m_G}\right)$ instead of $\left(\frac{m_G + 1}{m_G}\right)$ for internal gears.

VI. Coefficient of Friction

The coefficient of friction is the principal source of inaccuracy^[1] in these calculations. It depends upon:

- (a) The materials: Variations in the composition in the manufacture produce changes in the properties of the resulting gear causing marked variations in the coefficient of friction.
- (b) The accuracy: The accuracy of the tooth form and of the relative positioning in the gear casing are complementary. Errors of either kind result in localized tooth contact, and the excessive pressure which results may combine with relatively less favorable conditions over the actual areas of contact to produce an appreciable increase in coefficient of friction.
- (c) The surface finish condition: The type of finish, the smoothness, and the direction of cutting of the tool marks on the gear tooth profiles, influence the coefficient of friction appreciably.
- (d) The type of lubricant: Proper selection of the lubricant may decrease the coefficient of friction, it is related to the operating temperature and its viscosity.
- (e) The velocity of sliding: Experimental results show that the coefficient of friction is not independent of the sliding velocity. Therefore, for a given standard of materials, workmanship, and lubrication, the velocity of sliding is the most important controlling factor.
- (f) The surface stress condition: Under the satisfactory conditions of lubrication, increase in surface pressure tends to reduce the coefficient of friction, but increased loading of a given

gear assembly also produces deflection, which, by changing the mean position of tooth bearing, will mask the effect of change of pressure.

These factors can be investigated only by experiment, and since they are difficult to isolate, the present state of knowledge is incomplete.

Merritt^[1] suggests using $\mu = 0.08$ for steel gears; this value includes the loss, due to load, of ball or roller bearings of normal proportions. Shipley's^[6] test data shows that the coefficient of friction μ lies between 0.03 to 0.05 for 20° pressure angle, case-carburized and ground spur gears, with average lubrication fed in at 120°F inlet temperature, for a pitch line velocity range of 300 to 5,500 fpm at various load factors.^[2]

A further detailed study of the coefficient of friction is beyond the scope of this thesis. Judging from the values suggested by Merritt and the test data obtained by Shipley, it appears reasonable to use:

$\mu = 0.04$ for precision steel gears.

$\mu = 0.05$ for accurately cut steel gears.

when no adequate design data are obtainable by experiment for design purposes.

VII. Efficiency

Having those formulas for gear-tooth sliding friction power loss calculation, and the reasonable assumption of coefficient of friction described in preceding article, the efficiency η expressed in percentage can readily be calculated.

$$\eta = 100 \left(1 - \frac{P_f}{P_{in}} \right) \quad (30)$$

where

P_{in} = Power input

$$= W \cdot \frac{d_b}{2} \cdot \omega_p$$

Different cases have to be considered for contact ratio is taken into account.

Case 1. When contact ratio is between 1 and 2, i.e., $1 < m_p < 2$

Substitute Eq. (22) into Eq. (30) for external gears.

$$\eta = 100 - \mu \left\{ 100 \left(\frac{m_g+1}{m_g} \right) \frac{1}{d_b} \left[\frac{Z_a^2 + Z_r^2}{2 p_b} + \frac{(p_b - Z_a)^2 + (p_b - Z_r)^2}{2 p_b} \right] \right\} \quad (31)$$

This can be written

$$\eta = 100 - \mu \Delta_2 \quad (32)$$

where Δ_2 is the "tooth loss factor" and the subscript 2 denotes that the contact ratio is less than 2.

And Δ_2 is given by

$$\Delta_2 = 100 \left(\frac{m_g+1}{m_g} \right) \frac{1}{d_b} \left[\frac{Z_a^2 + Z_r^2}{2 p_b} + \frac{(p_b - Z_a)^2 + (p_b - Z_r)^2}{2 p_b} \right] \quad (33)$$

For internal gears, use $\left(\frac{m_g-1}{m_g} \right)$ instead of $\left(\frac{m_g+1}{m_g} \right)$.

If $Z_a > p_b$ or $Z_r > p_b$, the terms $(p_b - Z_a)^2$ and $(p_b - Z_r)^2$ should change signs respectively. (Refer to Eq. 22a and 22b)

Case 2. When contact ratio is between 2 and 3, i.e., $2 < m_p < 3$

Substitute Eq. (28) into Eq. (30) for external gears.

$$\eta = 100 - \mu \left\{ 100 \left(\frac{m_g + 1}{m_g} \right) \frac{1}{d_b} \left[\frac{Z_a^2 + Z_r^2}{3p_b} \right. \right. \\ \left. \left. + \frac{(2p_b - Z_a)^2 + (2p_b - Z_r)^2}{6p_b} - \frac{(Z_a - p_b)^2 + (Z_r - p_b)^2}{6p_b} \right] \right\} \quad (34)$$

This can be written

$$\eta = 100 - \mu \Delta_3 \quad (35)$$

where Δ_3 is the "tooth loss factor" and the subscript 3 denotes that the contact ratio is less than 3;

And Δ_3 is given by

$$\Delta_3 = 100 \left(\frac{m_g + 1}{m_g} \right) \frac{1}{d_b} \left[\frac{Z_a^2 + Z_r^2}{3p_b} \right. \\ \left. + \frac{(2p_b - Z_a)^2 + (2p_b - Z_r)^2}{6p_b} - \frac{(Z_a - p_b)^2 + (Z_r - p_b)^2}{6p_b} \right] \quad (36)$$

For internal gears, use $\left(\frac{m_g - 1}{m_g} \right)$ instead of $\left(\frac{m_g + 1}{m_g} \right)$.

If $p_b > Z_a$ or $p_b > Z_r$, the terms $(Z_a - p_b)^2$ and $(Z_r - p_b)^2$ should change sign respectively. (Refer to Eq. 28a).

Case 3. When the contact ratio happens to be an integer, both Eq. (31) and (34) for external gears will be reduced to the form

$$\eta = 100 - \mu \left\{ 100 \left(\frac{m_g + 1}{m_g} \right) \frac{1}{d_b} \left[\frac{Z_a^2 + Z_r^2}{Z_a + Z_r} \right] \right\} \quad (37)$$

which gives the same result as obtained by substituting Eq. (29) into Eq. (30).

This can also be written

$$\eta = 100 - \mu \Delta \quad (38)$$

where Δ is the "tooth loss factor" and without subscript denotes that the contact ratio is an integer,

And Δ is given by

$$\Delta = 100 \left(\frac{m_g + 1}{m_g} \right) \frac{1}{d_b} \left[\frac{Z_a^2 + Z_r^2}{Z_a + Z_r} \right] \quad (39)$$

In this case, no correction of sign is necessary, because the load distribution becomes constant all along the line of action.

For internal gears, use $\left(\frac{m_g - 1}{m_g} \right)$ instead of $\left(\frac{m_g + 1}{m_g} \right)$.

In this case 3, the Eq. (37) and (39) have the same form as the equations developed by Merritt^[1]. This is a particular case only, for in most of the practical cases, the contact ratio very seldom happens to be an integer.

The Eqs. (33) (36) and (39) may be put into another dimensionless form, by introducing the relations of standard gear teeth: (Fig. 1)

$$Z_a = \sqrt{\left(\frac{D_o}{2}\right)^2 - \left(\frac{D_p}{2}\right)^2} - \frac{D}{2} \sin \phi$$

$$= \frac{1}{2P_d} \left[\sqrt{(N_g + 2)^2 - (N_g \cos \phi)^2} - N_g \sin \phi \right]$$

$$Z_r = \sqrt{\left(\frac{d_o}{2}\right)^2 - \left(\frac{d_p}{2}\right)^2} - \frac{d}{2} \sin \phi$$

$$= \frac{1}{2P_d} \left[\sqrt{(N_p + 2)^2 - (N_p \cos \phi)^2} - N_p \sin \phi \right]$$

$$d_b = d \cos \phi = \frac{1}{P_d} N_p \cos \phi$$

$$D_b = D \cos \phi = \frac{1}{P_d} N_G \cos \phi$$

$$\phi_b = \frac{1}{P_d} \pi \cos \phi$$

$$\frac{m_g + 1}{m_g} = \frac{N_p + N_G}{N_G}$$

the Eqs. (33), (36) and (39) of tooth-loss factor Δ can be expressed in terms of the number of teeth N_p and N_G only. Therefore, by substituting various numbers of teeth for the pinion and gear, the corresponding value of the tooth loss factor Δ can be determined.

For full-depth standard teeth, 20° pressure angle, the tooth loss factor Δ_2 is plotted against the number of teeth in the pinion N_p and the number of teeth in the gear N_G , as shown in Fig. 20. Interference of tooth combinations are also shown in the shaded area.

Fig. 21 is the comparison of the tooth-loss factor with that developed by Merritt (the particular case where the contact ratio is an integer). From the results shown, in the figure, it is evident that the power loss calculated based on Merritt's equation is higher, and therefore the efficiency is lower.

A comparison of the power losses calculated by the method of the rigid tooth, the elastic tooth, and the Merritt's proposal are shown in Table 2; it alternatively shows the comparison of efficiencies. Sample calculation of one of the tooth combinations for 40-tooth pinion and 80-tooth gear is given in Appendix II.

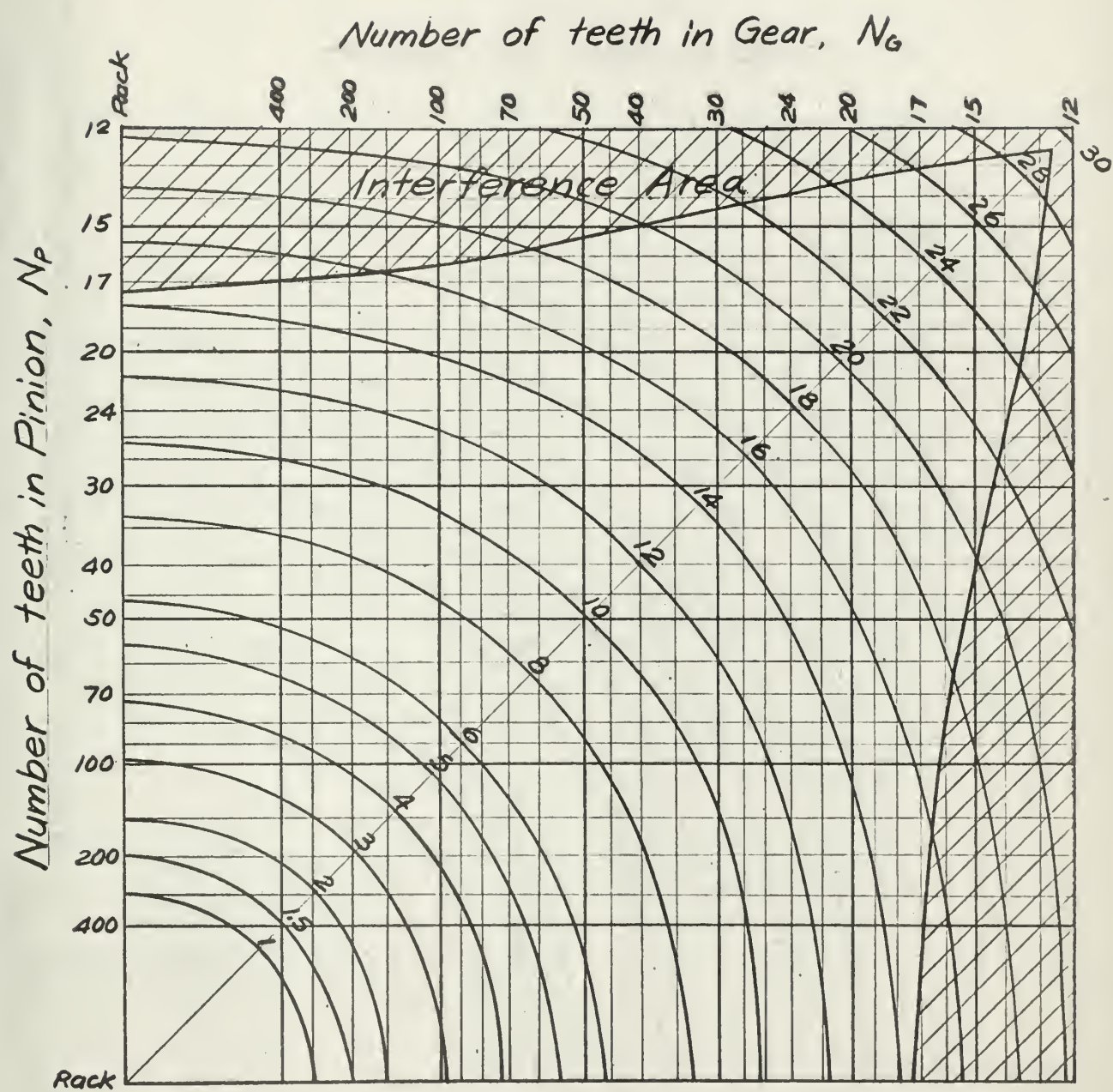


Fig. 20. Tooth loss factor of 20° full-depth spur gear.

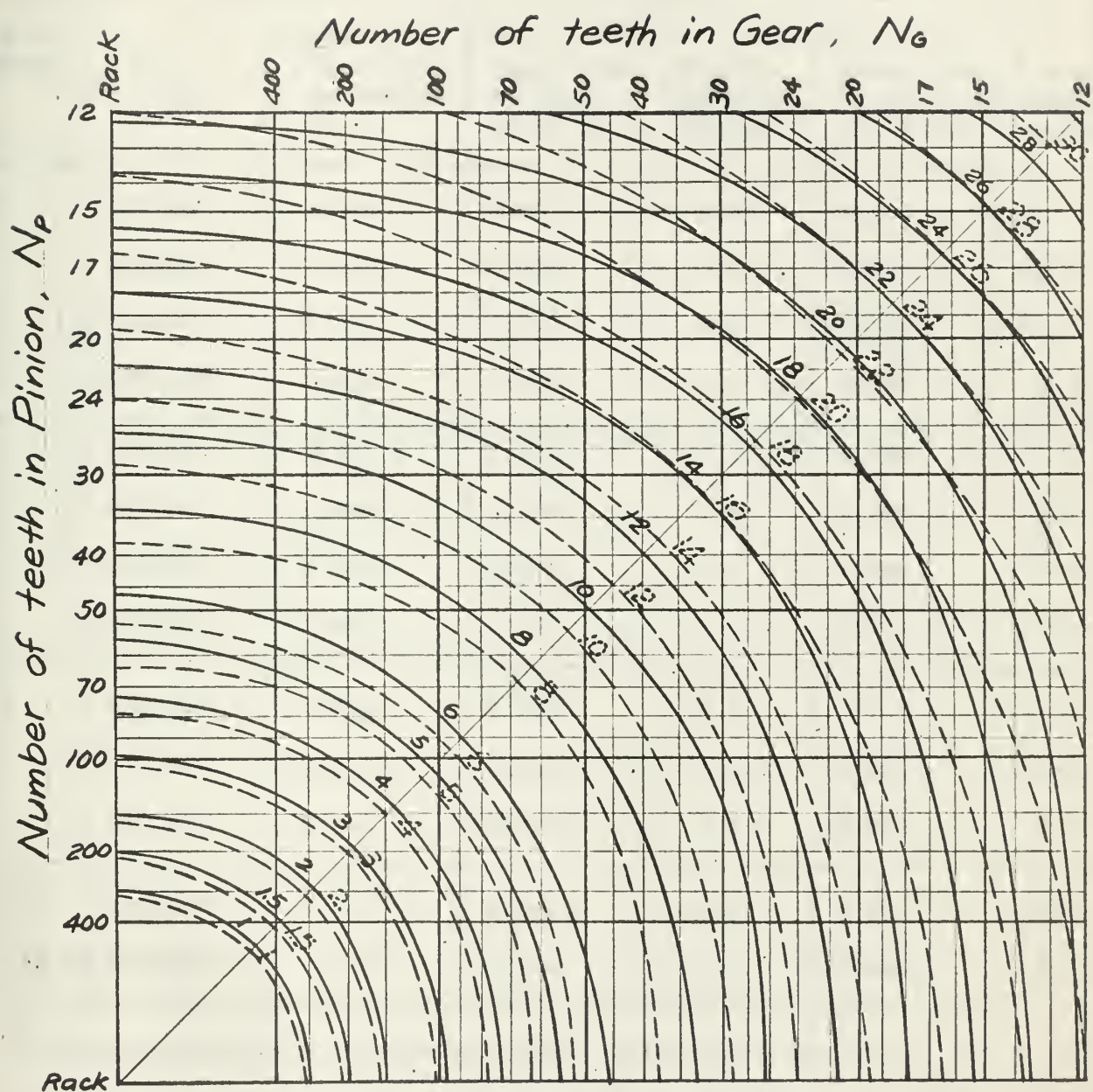


Fig. 21. Comparison of tooth loss factor of 20° full-depth spur gear with the results developed by Merritt shown in dotted lines.

TABLE 2

Comparison of gear tooth friction loss based on Merritt's Eq.

Gear Ratio	N_p/N_g	*** Power loss by Merritt Eq.	** Power loss by rigid tooth Eq.	% diff. based on Merritt's	* Power loss by elastic tooth Eq.	% diff. based on Merritt's
1	20T/20T	0.779	0.655	-15.9	0.644	-17.3
	40T/40T	0.858	0.755	-12.0	0.741	-13.7
	80T/80T	0.913	0.839	- 8.1	0.825	- 9.6
	100T/100T	0.926	0.860	- 7.1	0.846	- 8.6
2	20T/40T	0.821	0.705	-14.1	0.689	-16.1
	40T/80T	0.886	0.799	- 9.8	0.785	-11.4
	100T/200T	0.939	0.896	- 4.5	0.886	- 5.6
	200T/400T	0.963	0.931	- 3.3	0.925	- 4.0
5	20T/100T	0.859	0.760	-10.5	0.741	-13.9
	40T/200T	0.909	0.835	- 8.1	0.820	- 9.8
	80T/200T	0.943	0.893	- 5.2	0.882	- 6.5
10	20T/200T	0.878	0.786	-10.5	0.764	-13.0
	40T/400T	0.917	0.850	- 7.3	0.828	- 9.7

*** Calculated from the bracket of Eq. (29) or (39) divided by p_b .** Calculated from the bracket of Eq. (22) or (33) divided by p_o .* Calculated from the bracket of Eq. (26) divided by p_o .

VIII. Effect of Manufacturing Error:

All of the statements in the preceding articles are based upon the fact that the gear teeth are cut precisely, with no deviation in profile or spacing. Suppose that at point i in Fig. 6, deviations from the precise involute profiles of teeth P and G , or the spacing of the profile on the pinion is greater than that on the gear, have the effect of producing a gap ε at point i when contact occurs without load. Then under the action of a total load W , if λ_a and λ_r represent the combined stiffnesses at point i and b , all the load will be carried at b if $W < \varepsilon \lambda_r$.

If $W > \varepsilon \lambda_r$, the total load according to Merritt^[1] will be divided thus

$$w_a = \frac{W \cdot \lambda_a - \varepsilon \lambda_a \lambda_r}{\lambda_a + \lambda_r} \quad (40)$$

$$w_r = \frac{W \cdot \lambda_r + \varepsilon \lambda_a \lambda_r}{\lambda_a + \lambda_r} \quad (41)$$

From these two equations, we can see that a larger portion of the total load is carried by the teeth on the recess side. For the power loss determination, the load diagram for rigid teeth may also be applied to the elastic teeth. Let $+kW$ be the increase of load on the recess side and $-kW$ be the decrease of load on the approach side as shown in Fig. 22, then the average power loss can be expressed as follows:

$$P_f = \frac{1}{P_b} \left\{ \int_c^{p_b - z_a} \mu W \left[\left(\frac{m_g + 1}{m_s} \right) \omega_p s \right] ds + \int_0^{p_b - z_r} \mu W \left[\left(\frac{m_g + 1}{m_s} \right) \omega_p s \right] ds \right. \\ \left. + \int_{p_b - z_a}^{z_r} \mu \left(\frac{1}{2} + k \right) W \left[\left(\frac{m_g + 1}{m_s} \right) \omega_p s \right] ds + \int_{p_b - z_r}^{z_a} \mu \left(\frac{1}{2} - k \right) W \left[\left(\frac{m_g + 1}{m_s} \right) \omega_p s \right] ds \right\} \quad (42)$$

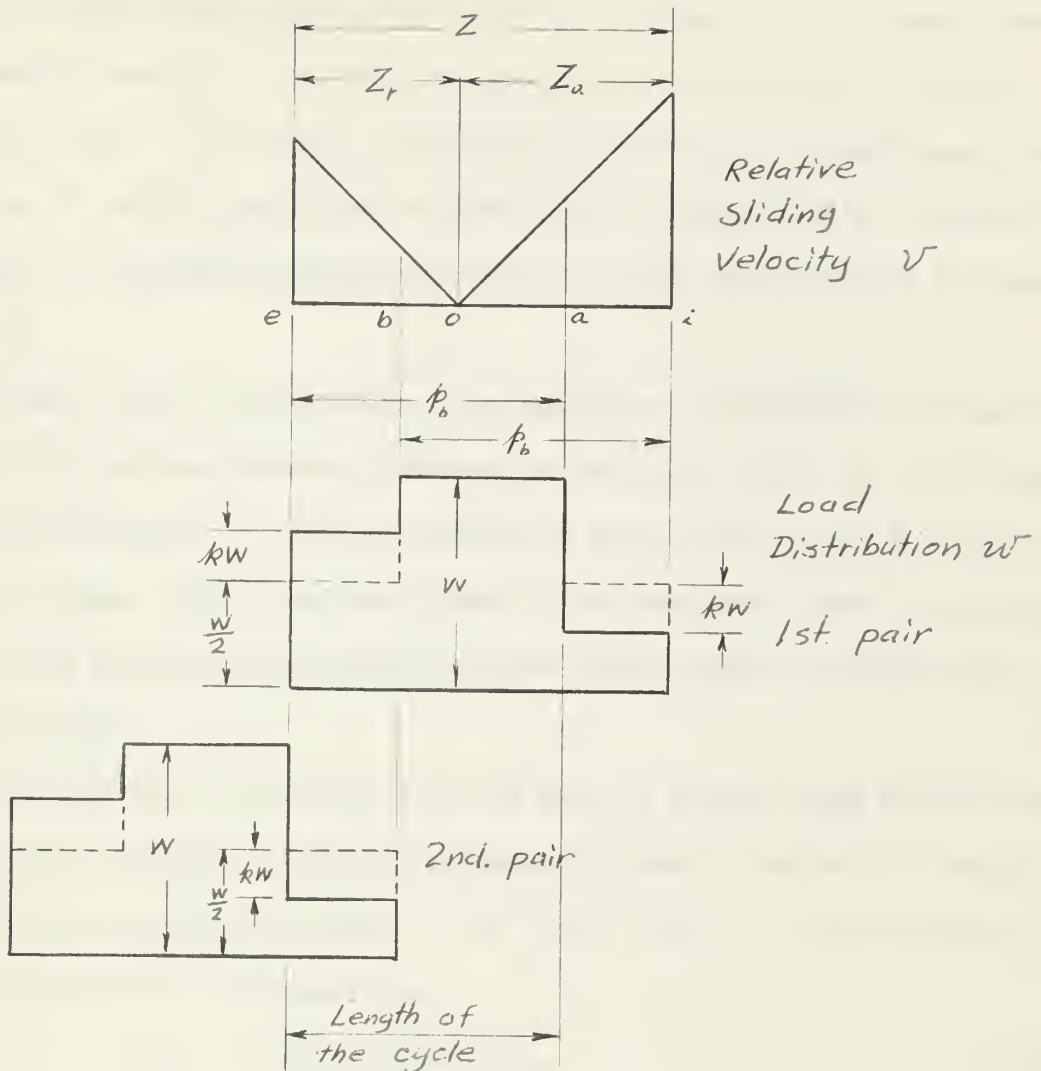


Fig. 22. Load distribution diagram for rigid tooth when deviation in profile or spacing occurs.

performing the integrals and simplifying; we have

$$P_f = \mu \frac{WW_p}{2} \left(\frac{m_g + 1}{m_g} \right) \left\{ \frac{Z_a^2 + Z_r^2}{2P_b} + \frac{(P_b - Z_a)^2 + (P_b - Z_r)^2}{2P_b} \right. \\ \left. + K \left[\frac{Z_r^2 - Z_a^2 + (P_b - Z_r)^2 - (P_b - Z_a)^2}{P_b} \right] \right\} \quad (43)$$

Comparing this equation with Eq. (22) we note additional terms containing K in the bracket.

For standard gear systems, the length of approach Z_a is always equal to or greater than Z_r , and from the systematic calculations, it can be shown that $|Z_r - Z_a| > |(\rho_b - z_r) - (\rho_b - z_a)|$. Therefore, the additional terms containing κ will be negative in sign. Thus the power loss is decreased when there is a uniform manufacturing error in each tooth spacing as shown in Fig. 22.

In case of gear teeth with modified addendum, the increased addendum of the pinion and the decreased addendum of the gear causes Z_r to be equal to or greater than Z_a , then the additional terms containing κ will be positive in sign. Thus, the power loss is increased when there is uniform manufacturing error in tooth spacing on the pinion which is greater than that on the gear.

If the spacing of the profile on the gear is greater than that on the pinion, that is the gap ε will be produced at point b in Fig. 6, and all the load will be carried at point i if $W < \varepsilon \lambda_a$. And if $W > \varepsilon \lambda_a$, the total load will be divided thus

$$w_a = \frac{W \lambda_a + \varepsilon \lambda_a \lambda_r}{\lambda_a + \lambda_r} \quad (44)$$

$$w_r = \frac{W \lambda_r - \varepsilon \lambda_a \lambda_r}{\lambda_a + \lambda_r} \quad (45)$$

The load distribution diagram of Fig. 22 will be reversed, i.e., a large portion of the total load is carried by the teeth on the approach side. The resulting power loss will thus also be reversed. Table 3 gives a summary of these results.

In each case considered in Table 3, if $Z_a = Z_r$, then the power loss will not be changed even though a uniform manufacturing error in tooth spacing is involved.

Table 3. Summary of the effect of uniform manufacturing error

Spacing		Pinion > Gear	Gear > Pinion
Power loss	Standard tooth	Decrease	Increase
	Modified tooth	Increase	Decrease

The amount of the power loss depends upon the magnitude of the actual manufacturing error produced on the pinion or on the gear.

IX. Practical Example

A gear box unit is used as an example to analyze and to show the comparison of calculated and the actual friction power loss due to gear tooth sliding, the gear box unit is designed and manufactured by Western Gear Corporation, the following gear data and test data are supplied by them:

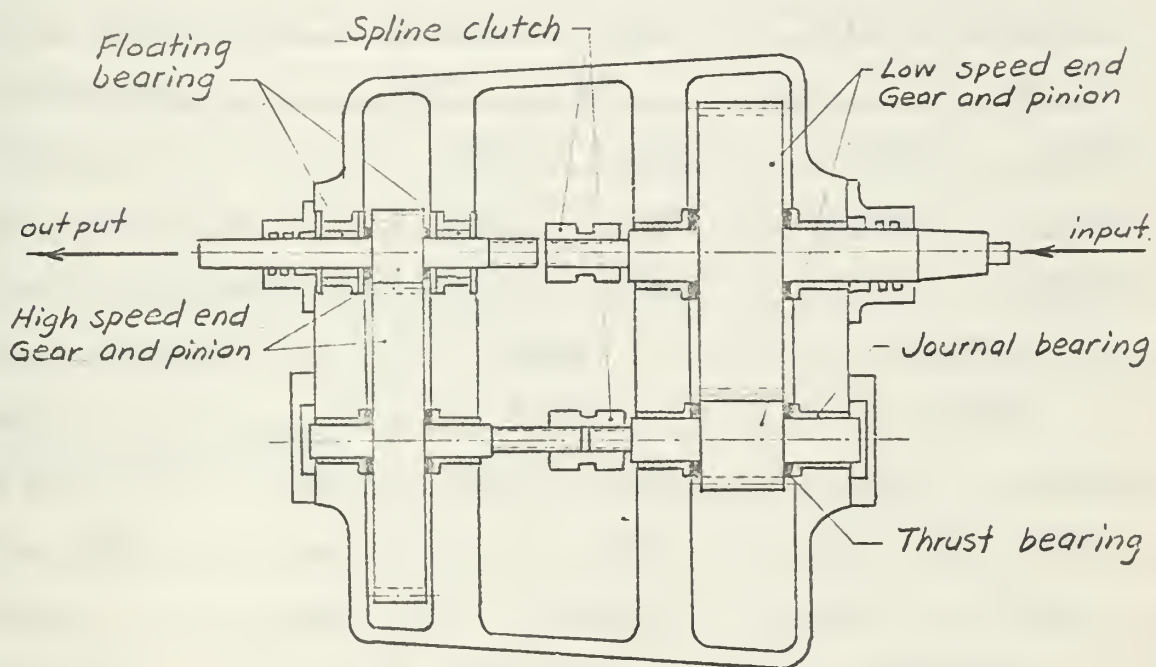


Fig. 23. General arrangement of a practical Gear box unit.

Test data:

Horse power	626.62 HP input, 582.06 HP output
Speed	4,500 RPM input, 60,750 RPM output
Lub. oil	Shell 2190 TEP (light turbine oil)
Oil temperature	150°F inlet, 256°F outlet.
Method of lubrication:	External source of 30 psi. pressure feed for bearings, spray for gear teeth and splines

Gear data

	Low speed		High speed	
	Pinion	Gear	Pinion	Gear
Number of teeth	23	58	17	91
Diametral pitch	6	6	8	8
Pitch diameter in.	3.833	9.667	2.125	11.375
Pressure angle	20°	20°	20°	20°
Addendum in.	.2500	.0835	.1650	.0850
Whole depth in.	.3917	.3917	.2938	.2938
Base circle diameter in.	3.6012	9.0835	1.9969	10.6890
Center distance in.	6.750		6.750	
Ratio	2.5217		5.3529	
(start of active profile) S.A.P. in.	.4152	1.0941	.1173	1.5845
Face width in.	4.75	4.44	2.50	2.19
Weight lb.	37	139.8	10.5	78.8
Material	AISI 4620		AISI 4620	
Hardness	Rc 60		Rc 60	

Detail calculations are given in the Appendix III.

Summary of analyzed results are tabulated as follows:

Journal bearing losses	22.22 HP
Thrust bearing losses	10.55 HP
Tooth sliding losses	8.08 HP
Windage and oil churning losses	2.44 HP
Other losses	1.36 HP
Total	44.65 HP

In this example, the tooth sliding losses are calculated as in case I in the previous article. It shows that the method of calculation of gear tooth sliding loss agrees closely with that of the actual conditions.

The other losses can be attributed to the uncertainty of the approximation of windage and oil churning losses which are calculated based on the method of turbine disc losses, and to the loss due to gear and spline teeth striking the oil particles when the oil is sprayed from the nozzles opposing the direction of the tooth velocity. A certain amount of energy is used to dissipate the kinetic energy of these oil particles. This loss cannot be calculated because of the unknown fraction of sprayed oil which is struck by the teeth, the approach and rebound direction and velocity of each oil particle when it is being struck.

Also, one of the thrust bearing losses due to the relative rotation of the end surface of the floating bearing is not included, because of large clearance, the loss can be neglected.

X. Conclusions

1. For practical elastic and precisely cut gear teeth, when two pairs of teeth are in contact simultaneously, the load is not equally distributed on each pair of teeth as it is considered for rigid teeth. The teeth take a lesser fraction of the total load at the beginning and at the end of contact increasing gradually to a greater fraction of the total load as they approach and depart from the region where a single pair of teeth are in contact. (Fig. 12)

2. The load distribution is a linear function of the distance from the pitch point to the point of contact when two pairs of teeth are in contact as shown from the results obtained by systematic calculations. The slope of the linear function differs for the different gear combinations. Generally, for the same gear ratio, the smaller the total number of teeth, the greater the slope. (Fig. 13 - 16)

3. For other standard gear systems with pressure angles of other than 20° , similar linear functions of load distribution would be expected.

4. Calculations show that the power loss due to tooth sliding friction based on elastic teeth is slightly less than those based on rigid teeth. This difference is small enough to be neglected (Table 2). Therefore, the tooth sliding friction power loss can be determined simply by treating the gear teeth as rigid. This assumption stands on the safe side from the design point of view.

5. The calculated results, as shown in Fig. 13, 14, 15 and 16, cover all the practical cases of gear teeth in combination. Some of the load distributions are not exactly symmetrical. This can also be neglected when the gear tooth sliding friction power loss is compared to the rigid teeth base.

6. Similar approximations to rigid teeth may also be applied in the case of 3 pairs of teeth in contact, which occurs in $14\frac{1}{2}^\circ$ full-depth teeth system.

7. The efficiency of rigid teeth with equally distributed load when more than one pair of teeth are in contact is higher than the efficiency for constant load distribution for the entire tooth action. The difference is large when the total number of teeth $N_p + N_G$ is small as shown in Table 2. This difference cannot be neglected. Therefore, for an efficiency calculation, the load carried by each pair of teeth when the contact ratio is not an integer should be taken into account. Merritt's development is true only when the contact ratio happens to be an integer.

8. From Fig. 21, it can be seen that the difference between the two methods becomes greater as the gear ratio approaches unity. It can also be seen from Table 2 that for the same number of teeth in the pinion, the difference decreases as the gear ratio increases.

9. The tooth loss factor curves shown in Fig. 21 are compared with those curves of Merritt's results. The values at upper right corner tend to coincide with each other. If this figure were constructed with the number of teeth starting from 10, it would be seen that when the tooth loss factor reaches 32, both results will be identical. This is due to the fact that in this region the Merritt's curves were constructed based on the addendum modification of British specifications to avoid interference.

10. Fig. 20 is constructed for 20° full-depth teeth only. Similar figures can be constructed for other pressure angles, and for stub teeth as well as for full-depth teeth in order to simplify the design work, if a standard tooth form is used.

11. Referring to Fig. 5 for $14\frac{1}{2}^\circ$ full-depth teeth, it is necessary to modify the addendum to avoid interference. From the practical point of

view for better operational results^[7], the contact ratio lies between 1.25 and 1.4. If the addendum is modified, the contact ratio, relative tooth sliding velocity, scoring factor and the efficiency will improve accordingly. Therefore, no charts or figures of tooth loss factor will be available for modified teeth. Calculations must be carried out according to suitable cases described in article VII. Whenever design work is proceeding, the necessary quantities for tooth loss factor calculations are not a tedious work.

12. The selection of the value of the coefficient of friction has a great effect on the power loss calculation. It may overshadow the effect due to gear tooth load distribution if a higher value of coefficient of friction is used. Reasonable assumption of μ must be made when no adequate test data are available. Comparisons of power loss for different methods of calculation are independent of the value of the coefficient of friction.

13. The effect of manufacturing error as described in Article IX depends on the length of approach, length of recess and whether the error produced is uniformly distributed on the gear or the pinion.

BIBLIOGRAPHY

1. H. E. Merritt, "Gears", Third Edition 1954, Reprinted 1961, Sir Issac Pitman & Sons, Ltd. London.
2. D. W. Dudley, "Practical Gear Design", First Edition 1954, McGraw-Hill Book Co., Inc., New York.
3. E. K. Gatcombe, R. W. Prowell, "Rocket Motor-Gear Tooth Analysis--Hertzian Contact Stresses and Times", ASME Transactions, Series B, Vol. 82, Aug. 1960, pp. 223.
4. H. Walker, "Gear Tooth Deflection and Profile Modification", The Engineer, Vol. 166, 14th and 21st Oct. 1938, pp. 409-412, 434-436.
5. H. Walker, "Gear Tooth Deflection and Profile Modification", The Engineer, Vol. 170, 16th Aug. 1940, pp. 102-103.
6. E. E. Shipley, "How to Predict Efficiency of Gear Trains", Product Engineering, 4th Aug. 1958, pp. 44-45.
7. V. M. Faires, "Design of Machine Elements", 3rd edition, The MacMillan Co., New York, 1955.

APPENDIX I

SAMPLE CALCULATIONS OF GEAR TOOTH LOAD DISTRIBUTION

Given: Standard full-depth involute tooth form

$$\text{Number of teeth in Pinion} \quad N_p = 40$$

$$\text{Number of teeth in Gear} \quad N_G = 80$$

$$\text{Pressure angle} \quad \phi = 20^\circ$$

Calculations:

$$\phi = 20^\circ = 0.34907 \text{ rad.}$$

$$\text{use } P_d = 1$$

$$f_b = \frac{\pi \cos \phi}{P_d} = \pi \cos \phi = 2.95212 \text{ in.}$$

Pinion

$$d = \frac{N_p}{P_d} = \frac{40}{1} = 40 \text{ in.}$$

$$d_o = \frac{N_p + 2}{P_d} = \frac{40 + 2}{1} = 42 \text{ in.}$$

$$d_R = \frac{N_p - 2.314}{P_d} = \frac{40 - 2.314}{1} = 37.6860 \text{ in.}$$

$$r_R = \frac{d_R}{2} = 18.8430 \text{ in.}$$

$$d_b = d \cos \phi = 40 \times 0.93969 = 37.5876 \text{ in}$$

$$r_b = \frac{d_b}{2} = 18.7938 \text{ in.}$$

$$\phi - \frac{\pi}{2N_p} = 0.34907 - \frac{\pi}{80} = 0.30980 \text{ rad.}$$

$$\text{Inv } \phi = \tan \phi - \phi = 0.36397 - 0.34907$$

$$= 0.01490 \text{ rad.}$$

$$\text{Inv } \delta_p^l = \frac{\sqrt{r_R^2 - r_b^2}}{r_b} - \tan^{-1} \frac{\sqrt{r_R^2 - r_b^2}}{r_b}$$

$$= \frac{\sqrt{18.843^2 - 18.7938^2}}{18.7938} - \tan^{-1} \frac{\sqrt{18.843^2 - 18.7938^2}}{18.7938} = 0.00015 \text{ rad.}$$

$$\delta_p = d_r \left[\frac{\pi}{2N_p} + (\text{Inv } \phi - \text{Inv } \delta_p^l) \right] = 1.98634 \text{ in.}$$

Gear:

$$D = \frac{N_G}{P_d} = \frac{80}{1} = 80 \text{ in.}$$

$$D_o = \frac{N_G+2}{P_d} = \frac{80+2}{1} = 82 \text{ in.}$$

$$D_R = \frac{N_G - 2.314}{P_d} = \frac{80 - 2.314}{1} = 77.6860 \text{ in.}$$

$$R_R = \frac{D_R}{2} = 38.8430 \text{ in}$$

$$D_b = D \cos \phi = 80 \times 0.43969 = 75,1752 \text{ in.}$$

$$R_b = \frac{D_b}{2} = 37.5876 \text{ in.}$$

$$\phi - \frac{\pi}{2N_G} = 0.34907 - \frac{\pi}{76} = 0.33043 \text{ rad.}$$

$$\operatorname{Inv} \phi = 0.01490 \text{ rad.}$$

$$\operatorname{Inv} \delta_G^L = \frac{\sqrt{R_R^2 - R_b^2}}{R_b} - \tan^{-1} \frac{\sqrt{R_R^2 - R_b^2}}{R_b}$$
$$= 0.00573 \text{ rad.}$$

$$t_G = D_r \left[\frac{\pi}{2N_G} + (\operatorname{Inv} \phi - \operatorname{Inv} \delta_G^L) \right]$$

$$= 2.23842 \text{ in.}$$

Length of approach:

$$Z_a = \frac{1}{2} \left[\sqrt{D_o^2 - D_b^2} - D \sin \phi \right]$$

$$= \frac{1}{2} \left[\sqrt{82^2 - 75,1752^2} - 80 \times 0.34202 \right]$$

$$= 2.69157 \text{ in.}$$

Length of recess:

$$Z_r = \frac{1}{2} \left[\sqrt{D_o^2 - D_b^2} - d \sin \phi \right]$$

$$= \frac{1}{2} \left[\sqrt{82^2 - 37,5876^2} - 40 \times 0.34202 \right] = 2.52939 \text{ in.}$$

Contact ratio:

$$m_p = \frac{Z}{p_b} = \frac{2.69517 + 2.52939}{2.95212} = 1.76977$$

Combined stiffness: Eq. (11) and (12)

$$\lambda_r = \frac{E/K}{\left[\frac{r_b}{t_p} - \frac{r_a}{t_p} \cos(\phi - \frac{\pi}{2N_p} + \frac{s}{r_b}) \right] + \left[\frac{R_b}{t_g} - \frac{R_a}{t_g} \cos(\phi - \frac{\pi}{2N_g} - \frac{s}{R_b}) \right]}$$

$$= \frac{E/K}{26.25354 - \left[9.48881 \cos(0.30980 + 0.05321S) + 17.35510 \cos(0.33043 - 0.02661S) \right]}$$

$$\lambda_a = \frac{E/K}{\left[\frac{r_b}{t_p} - \frac{r_a}{t_p} \cos(\phi - \frac{\pi}{2N_p} + \frac{s-p_a}{r_b}) \right] + \left[\frac{R_b}{t_g} - \frac{R_a}{t_g} \cos(\phi - \frac{\pi}{2N_g} - \frac{s-p_a}{R_b}) \right]}$$

$$= \frac{E/K}{26.25354 - \left[9.48881 \cos(0.15272 + 0.05321S) + 17.35510 \cos(0.40897 - 0.02661S) \right]}$$

Let $\lambda_r = \frac{E/K}{X}$ and $\lambda_a = \frac{E/K}{Y}$

then, Eq. (14) $W_r = \frac{\lambda_r}{\lambda_a + \lambda_r} \cdot W = \frac{Y}{X+Y} \cdot W \quad \therefore \frac{W_r}{W} = \frac{Y}{X+Y}$

Let $A = 0.30980 + 0.05321S$ } in X

$$B = 0.33043 - 0.02661S$$

$$C = 0.15272 + 0.05321S \quad } \quad \text{in } Y$$

$$D = 0.40897 - 0.02661S \quad }$$

S varies from $p_a - Z_a = 0.25695$ to $Z_r = 2.52939$

S	0.25695	1.00000	1.50000	2.00000	2.52939
A	0.32347	0.36301	0.38962	0.41622	0.44439
cos A	0.94813	0.93484	0.92506	0.91463	0.90287
9.48881 cos A	8.99663	8.87052	8.77772	8.67875	8.56716
B	0.32359	0.30382	0.29052	0.27721	0.26312
cos B	0.94810	0.95421	0.95810	0.96183	0.96559
17.35510 cos B	16.45437	16.56040	16.62792	16.69267	16.75791
X	0.80154	0.82262	0.84790	0.88212	0.92847
C	0.16639	0.20593	0.23254	0.25914	0.28731
cos C	0.98619	0.97888	0.97309	0.96662	0.95910
9.48881 cos C	9.35777	9.2881	9.23347	9.17207	9.09986
D	0.40213	0.38236	0.36906	0.35575	0.34166
cos D	0.92024	0.92777	0.93265	0.93737	0.94218
17.35510 cos D	15.97086	16.10154	16.18623	16.26815	16.35193
Y	0.92491	0.86359	0.83384	0.81332	0.80175
X + Y	1.72645	1.68621	1.68174	1.69544	1.73022
$\frac{w_r}{w}$	0.53573	0.51215	0.49582	0.47971	0.46338

APPENDIX II

COMPARISON OF FRICTION LOSS DUE TO TOOTH SLIDING

Given: Standard full-depth involute tooth form

Number of teeth in Pinion $N_p = 40$

Number of teeth in Gear $N_G = 80$

Pressure angle $\phi = 20^\circ$

Calculations:

From Appendix I, we have

base pitch $p_b = 2.95212 \text{ in.}$

length of approach $Z_a = 2.69515 \text{ in.}$

length of recess $Z_r = 2.52939 \text{ in.}$

$$Z_a = \frac{2.69515}{2.95212} p_b = 0.913 p_b$$

$$Z_r = \frac{2.52939}{2.95212} p_b = 0.858 p_b$$

Merritt's equation of friction power loss of Eq. (29), i.e.,
the particular case of constant load throughout the contact
length when the contact ratio is an integer.

$$\begin{aligned} P_f &= \mu \frac{W\omega_p}{2} \left(\frac{m_G+1}{m_G} \right) \left[\frac{Z_a^2 + Z_r^2}{Z_a + Z_r} \right] \\ &= \mu \frac{W\omega_p}{2} \left(\frac{m_G+1}{m_G} \right) \left[\frac{(0.913)^2 + (0.858)^2}{0.913 + 0.858} \right] p_b \\ &= \mu \frac{W\omega_p}{2} \left(\frac{m_G+1}{m_G} \right) [0.886 p_b] \end{aligned}$$

Rigid teeth power loss when contact ratio is between 1 and 2.

Eq. (22)

$$P_f = \mu \frac{W\omega_p}{2} \left(\frac{m_G+1}{m_G} \right) \left[\frac{Z_a^2 + Z_r^2}{2p_b} + \frac{(p_b - Z_a)^2 + (p_b - Z_r)^2}{2p_b} \right]$$

$$\begin{aligned}
 &= \mu \frac{W\omega_p}{2} \left(\frac{m_g+1}{m_g} \right) \left[\frac{(0.913)^2 + (0.858)^2}{2} + \frac{(0.087)^2 + (0.142)^2}{2} \right] p_b \\
 &= \mu \frac{W\omega_p}{2} \left(\frac{m_g+1}{m_g} \right) [0.799 p_b]
 \end{aligned}$$

Elastic teeth power loss when contact ratio is between 1 and

2. Eq. (26). $\epsilon = 0.036$ taken from Fig. 14.

The additional term containing ϵ is

$$\begin{aligned}
 &- \epsilon \frac{2}{3p_b} (Z_a + Z_r - p_b)^2 \\
 &= -0.036 \frac{2}{3p_b} (0.913 + 0.858 - 1)^2 p_b^2 \\
 &= -0.0144 p_b
 \end{aligned}$$

$$\begin{aligned}
 \text{Then } P_f &= \mu \frac{W\omega_p}{2} \left(\frac{m_g+1}{m_g} \right) [0.799 p_b - 0.0144 p_b] \\
 &= \mu \frac{W\omega_p}{2} \left(\frac{m_g+1}{m_g} \right) [0.785 p_b]
 \end{aligned}$$

Comparison of power loss for elastic teeth versus rigid teeth,

(rigid teeth as the base):

$$\% \text{ diff.} = \frac{0.785 - 0.799}{0.799} \times 100 = -1.8 \%$$

Comparison of power loss for elastic teeth with Merritt's

equation (Merritt's equation as the base):

$$\% \text{ diff.} = \frac{0.785 - 0.886}{0.886} \times 100 = -11.4 \%$$

Comparison of power loss for rigid teeth with Merritt's equa-

tion (Merritt's equation as the base):

$$\% \text{ diff.} = \frac{0.799 - 0.886}{0.886} \times 100 = -9.8 \%$$

APPENDIX III

DETAIL CALCULATIONS ON THE PRACTICAL EXAMPLE ANALYSIS

Referring to Fig. 23 of the General arrangement of the gear box unit, the test data and gear data given in article VIII, the power losses in the journal bearings, thrust bearings, tooth sliding, windage and oil churning are analyzed as follows:

(A) Journal bearings:

The analysis of power loss due to journal bearing is based on the method introduced by Wilcock and Booser "Bearing Design and Application" 1st edition, McGraw-Hill Book Co. Inc., 1957, for circumferential-groove full cylindrical bearings described on pp. 245-248.

(i) Low-speed gear bearings:

$$\text{Bearing dia. } D_{max.} = 3.5005" \quad D_{min.} = 3.5000"$$

$$\text{average } D = 3.5003"$$

$$\text{Shaft dia. } D_{max.} = 3.4950" \quad D_{min.} = 3.4945"$$

$$\text{average } D = 3.4948"$$

$$\text{Clearance } C = 3.5003 - 3.4948 = 0.0055"$$

$$\text{Length of bearing (over-all)} = 2.75"$$

$$\text{Groove width} = 0.3125"$$

$$\text{Length of bearing (individual)} L = \frac{2.75 - 0.3125}{2} = 1.2185"$$

$$\text{Length-diameter ratio } \frac{L}{D} = \frac{1.2185}{3.5} = 0.347$$

$$\text{Light turbine oil outlet temperature } f_2 = 256^{\circ}\text{F}$$

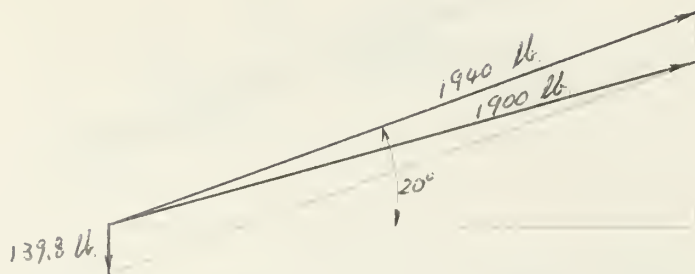
$$\text{SUS} = 38 \text{ sec.} \quad \therefore Z_2 = 2.93 \text{ cp.}$$

$$\text{Shaft speed, } N = 4,500 \text{ RPM}$$

Normal force on gear tooth (based on power input)

$$F = \frac{63000 \text{ HP}}{R_b \times N} = \frac{63000 \times 626.62}{\left(\frac{9.667}{2} \text{ cm}^2\right) \times 4500} = 1940 \text{ lb}$$

Weight of gear and shaft $W = 139.8$ lb



Bearing reaction $R = \frac{1900}{4} = 475$ lb.

Bearing area $A = 3.5 \times 1.2185 = 4.26 \text{ in}^2$

Bearing pressure $P = \frac{475}{4.26} = 111.5 \text{ psi.}$

Sommerfeld number

$$S = 2.42 \times 10^{-9} \left(\frac{D}{c} \right)^2 \frac{Z_2 N}{P}$$

$$= 2.42 \times 10^{-9} \left(\frac{3.5}{0.0055} \right)^2 \frac{2.93 \times 4500}{111.5} = 0.116$$

Power loss coefficient

$$j = \frac{f\left(\frac{D}{c}\right) \text{ by Fig. 7-20}}{f\left(\frac{D}{c}\right) \text{ by Fig. 7-19}} = \frac{5.2}{2.4} = 2.16$$

Total power loss

$$H = 3.79 \times 10^{-13} j \frac{N^2 D^3 L Z_2}{c}$$

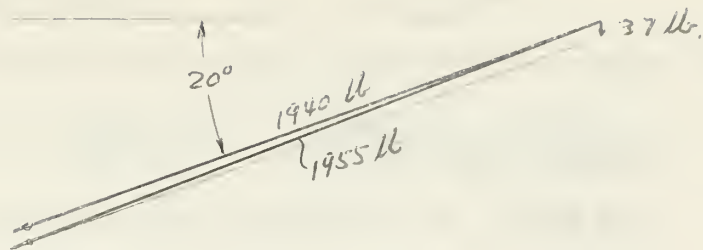
$$= 3.79 \times 10^{-13} \times 2.16 \frac{(4500)^2 (3.5)^3 (4 \times 1.2185) (2.93)}{0.0055} = 1.85 \text{ HP}$$

(iii) Low-speed pinion bearings:

Same dimensions as the bearings of low-speed gear.

Shaft speed $N = 4,500 \times 2.5217 = 11,350 \text{ RPM.}$

Weight of pinion and shaft $W = 37 \text{ lb.}$



Bearing reaction $R = \frac{1955}{4} = 489 \text{ lb.}$

Bearing pressure $P = \frac{489}{4.26} = 115 \text{ psi}$

Sommerfeld number

$$S = 2.42 \times 10^{-9} \left(\frac{D}{C} \right)^2 \frac{Z \cdot N}{P}$$

$$= 2.42 \times 10^{-9} \left(\frac{3.5}{0.0055} \right)^2 \frac{2.93 \times 11350}{115} = 0.284$$

Power loss coefficient

$$j = \frac{f(\frac{D}{C}) \text{ by Fig. 7-2c}}{f(\frac{D}{C}) \text{ by Fig. 7-19}} = \frac{8.3}{5.9} = 1.41$$

Total power loss

$$H = 3.79 \times 10^{-13} \cdot j \cdot \frac{N^2 D^3 L Z_2}{C}$$

$$= 3.79 \times 10^{-13} \times 1.41 \cdot \frac{(11350)^2 (3.5)^3 (4 \times 1.2185) (2.93)}{0.0055} = 7.61 \text{ HP}$$

(iii) High-speed gear bearings:

Bearing dia. $D_{max} = 2.6255'' \quad D_{min} = 2.6250''$

average $D = 2.6253''$

Shaft dia. $D_{max} = 2.6200'' \quad D_{min} = 2.6195''$

average $D = 2.6193''$

Clearance $C = 2.6253 - 2.6193 = 0.0060''$

Length of bearing (over-all) = 2.00"

Groove width = 0.3125"

Length of individual bearing $L = \frac{2.00 - 0.3125}{2} = 0.844''$

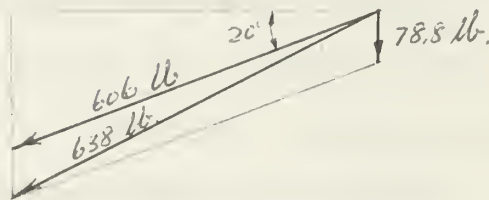
Length-diameter ratio $\frac{L}{D} = \frac{0.844}{2.6193} = 0.344$

Shaft speed $N = 11,350$ RPM

Normal force on gear tooth (based on output power)

$$F = \frac{63000 \text{ HP}}{R_b \times N} = \frac{63000 \times 582,06}{\left(\frac{11.375}{2} \cos 20^\circ\right) \times 11350} = 606 \text{ lb.}$$

Weight of gear and shaft $W = 78.8 \text{ lb.}$



$$\text{Bearing reaction } R = \frac{638}{4} = 159.5 \text{ lb.}$$

$$\text{Bearing area } A = 2.625 \times 0.844 = 2.22 \text{ in}^2$$

$$\text{Bearing pressure } P = \frac{159.5}{2.22} = 71.8 \text{ psi}$$

Sommerfeld number

$$S = 2.42 \times 10^{-9} \left(\frac{D}{c}\right)^2 \frac{Z_2 N}{P}$$

$$= 2.42 \times 10^{-9} \left(\frac{2.625}{0.006}\right)^2 \frac{2.93 \times 11350}{71.8} = 0.215$$

Power loss coefficient

$$j = \frac{f\left(\frac{P}{c}\right) \text{ by Fig. 7-20}}{f\left(\frac{P}{c}\right) \text{ by Fig 7-19}} = \frac{7.0}{4.4} = 1.59$$

Total power loss

$$H = 3.79 \times 10^{-13} j \frac{N^2 D^3 L Z_2}{c}$$

$$= 3.79 \times 10^{-13} \times 1.59 \frac{(11350)^2 (2.625)^3 (4 \times 0.844) (2.93)}{0.006} = 2.32 \text{ hp}$$

(iv) High-speed pinion floating bearings:

Bearing dia. $D_{max} = 1.7505''$; $D_{min} = 1.7500''$

average $D = 1.7503''$

Shaft dia. $D_{max} = 1.7400"$ $D_{min} = 1.7395"$

average $D = 1.7398"$

Clearance $C = 1.7503 - 1.7398 = 0.0105"$

Length of bearing (over-all) = 1.75"

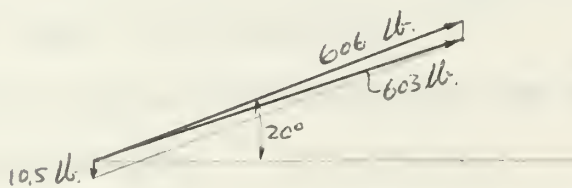
Groove width = 0.125"

Length of individual bearing $L = \frac{1.75 - 0.125}{2} = 0.813"$

Length-diameter ratio $\frac{L}{D} = \frac{0.813}{1.75} = 0.463$

Shaft speed $N = 30,375$ RPM. relative to bearing.

Weight of pinion and shaft $W = 10.5$ lb.



Bearing reaction $R = \frac{603}{4} = 151$ lb

Bearing area $A = 1.75 \times 0.81 = 1.425$ in²

Bearing pressure $P = \frac{151}{1.425} = 106$ psi

Sommerfeld number

$$S = 2.42 \times 10^{-9} \left(\frac{D}{C}\right)^2 \frac{Z_2 N}{P}$$

$$= 2.42 \times 10^{-9} \left(\frac{1.75}{0.0105}\right)^2 \frac{2.93 \times 30375}{106} = 0.0565$$

Power loss coefficient

$$j = \frac{f(\frac{P}{C}) \text{ by Fig. 7-20}}{f(\frac{P}{C}) \text{ by Fig. 7-19}} = \frac{2.9}{1.18} = 2.56$$

Total power loss

$$H = 3.79 \times 10^{-13} \cdot j \cdot \frac{N D^3 L Z_2}{C}$$

$$= 3.79 \times 10^{-13} \times 2.56 \frac{(30375)^2 (1.75)^3 (4 \times 0.813) (2.93)}{0.0105} = 2.48 \text{ HP}$$

(v) High-speed pinion stationary bearings:

Bearing dia. $D_{max.} = 2.2455"$ $D_{min.} = 2.2450"$

average $D = 2.2453"$

Shaft dia. $D_{max.} = 2.2400"$ $D_{min.} = 2.2395"$

average $D = 2.2398"$

Clearance $C = 2.2435 - 2.2398 = 0.0055"$

Length of bearing (over-all) = 1.75"

Groove width = 0.125"

Length of individual bearing $L = \frac{1.75 - 0.125}{2} = 0.813"$

Length-diameter ratio $\frac{L}{D} = \frac{0.813}{2.24} = 0.361$

Shaft speed $N = 30,375$ RPM

Bearing reaction can be treated as same as the floating bearing. $R = 151$ lb.

Bearing area $A = 2.24 \times 0.813 = 1.82 \text{ in}^2$

Bearing pressure $P = \frac{151}{1.82} = 83 \text{ psi}$

Sommerfeld number

$$S = 2.42 \times 10^{-9} \left(\frac{D}{C} \right)^2 \frac{Z_e N}{P}$$

$$= 2.42 \times 10^{-9} \left(\frac{2.24}{0.0055} \right)^2 \frac{2.93 \times 30375}{83} = 0.428$$

Power loss coefficient

$$j = \frac{f(\frac{D}{C}) \text{ by Fig. 7-20}}{f(\frac{P}{C}) \text{ by Fig. 7-19}} = \frac{10.1}{8.7} = 1.16$$

Total power loss

$$H = 3.79 \times 10^{-13} j \frac{N^2 D^3 L Z_e}{C}$$

$$= 3.79 \times 10^{-13} \times 1.16 \frac{(30375)^2 (2.24)^3 (4 \times 0.813) (2.93)}{0.0055} = 7.9 \text{ HP}$$

Summary of power loss of journal bearings:

Low-speed gear	1.85 HP
----------------	---------

Low-speed pinion	7.76 HP
High-speed gear	2.32 HP
High-speed pinion (floating)	2.48 HP
<u>High-speed pinion (stationary)</u>	<u>7.90 HP</u>
	Total 22.22 HP

(B) Thrust bearings:

The thrust bearings in this gear box are used for positioning only, there are no thrust load actually applied on them. To analyze the power loss due to thrust bearings with no load, a chart is given in the Wilcock and Booser's "Bearing Design and Application" 1st edition, McGraw-Hill Book Co. Inc., 1957, for flat-plate thrust bearings, described on pp. 315-316.

The equation for power loss is

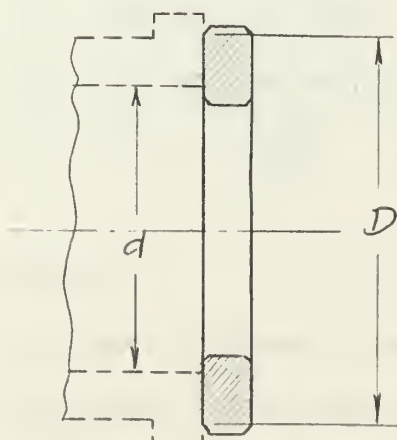
$$H = A \cdot M$$

where $A = \text{net thrust area} = \frac{\pi}{4} (D^2 - d^2) - \text{groove area, in}^2$

$M = \text{HP per square inch obtained by Fig. 11-1.}$

plotted against mean peripheral speed U

$$U = \frac{\pi}{12} \left(\frac{D+d}{2} \right) N \quad \text{ft/min.}$$



Dimensions are taken from drawings supplied by Western Gear Co.

The results are tabulated as follows:

Bearing location	No. of bearing	D in.	d in.	A in ²	N RPM	U fpm	M HP/in ²	H HP
Low speed gear	2	4.335	3.592	4.671	4,500	4,660	0.085	0.75
Low speed pinion	2	4.335	3.592	4.671	11,350	11,750	0.65	6.08
High speed gear	2	3.480	2.716	3.701	11,350	9,140	0.42	3.11
High speed pinion	2	2.345	1.832	1.554	60,750	33,300	*2.34	7.27
* This value obtained by extrapolation, The curve is straight at end of the curve.							Total	17.21

The chart of power loss per square inch of Fig. 11-1 in Wilcock and Booser's book is constructed based on the use of a medium-viscosity turbine oil. In case of this example, the oil used is light turbine oil. It is necessary to correct the power loss corresponding to light turbine oil condition. Other conditions remaining unchanged, the power loss is directly proportional to the viscosity. Therefore

$$\text{at } T_2 = 256^\circ\text{F} \quad Z_2 = 2.93 \text{ cp. for light turbine oil.}$$

$$Z_2 = 4.80 \text{ cp. for medium turbine oil.}$$

$$\therefore \text{Total power loss } H = 17.21 \times \frac{2.93}{4.80} = 10.55 \text{ HP}$$

(C) Gear Tooth sliding:

The analysis of power loss due to gear tooth sliding is based on the method obtained in this thesis. Referring to the gear data in article VIII.

(i) Low-speed gear and pinion:

$$p_o = \frac{\pi c \cos \phi}{P_d} = \frac{\pi c \cos 20^\circ}{6} = 0.4921 \text{ in}$$

$$Z_a = R \sin \phi - S.A.P.G$$

$$= \frac{9.667}{2} \sin 20^\circ - 1.0941 = 0.5591 \text{ in.}$$

$$Z_r = r \sin \phi - S.A.P.P$$

$$= \frac{3.833}{2} \sin 20^\circ - 0.4152 = 0.2403 \text{ in.}$$

Contact ratio: $m_p = \frac{Z_a + Z_r}{p_o} = \frac{0.5591 + 0.2403}{0.4921} = 1.625$

$$d_b = d \cos \phi = 3.833 \cos 20^\circ = 3.6018 \text{ in.}$$

$$\frac{m_G + 1}{m_G} = \frac{2.5217 + 1}{2.5217} = 1.3966$$

Use Eq. (33) and in case of $Z_a > p_o$

$$\Delta_2 = 100 \left(\frac{m_G + 1}{m_G} \right) \frac{1}{d_b} \left[\frac{Z_a^2 + Z_r^2}{2 p_o} + \frac{(p_o - Z_r)^2 - (p_o - Z_a)^2}{2 p_o} \right]$$

$$= 100 \times 1.3966 \times \frac{1}{3.6018} \left[\frac{0.3120 + 0.0575}{2 \times 0.4921} + \frac{0.0632 - 0.0045}{2 \times 0.4921} \right]$$

$$= 16.9$$

Percentage of power loss: use $\mu = 0.04$

$$\mu \Delta_2 = 0.04 \times 16.9 = 0.676 \%$$

power loss based on power input

$$P_f = \frac{0.676}{100} \times 626.62 = 4.23 \text{ HP}$$

(ii) High-speed gear and pinion:

$$p_o = \frac{\pi c \cos \phi}{P_d} = \frac{\pi c \cos 20^\circ}{8} = 0.3690 \text{ in.}$$

$$Z_a = R \sin \phi - S.A.P.G$$

$$= \frac{11.375}{2} \sin 20^\circ - 1.5845 = 0.3607 \text{ in.}$$

$$Z_r = r \sin \phi - S.A.P.P$$

$$= \frac{2.125}{2} \sin 20^\circ - 0.1173 = 0.2461 \text{ in.}$$

$$\text{Contact ratio: } m_p = \frac{0.3607 + 0.2461}{0.3690} = 1.645$$

$$d_b = d \cos \phi = 2.125 \cos 20^\circ = 1.9968 \text{ in.}$$

$$\frac{m_G + 1}{m_G} = \frac{5.3529 + 1}{5.3529} = 1.1868$$

Use Eq. (33).

$$\begin{aligned} \Delta_2 &= 100 \left(\frac{m_G + 1}{m_G} \right) \frac{1}{d_b} \left[\frac{Z_a^2 + Z_r^2}{2 P_b} + \frac{(P_b - Z_a)^2 + (P_b - Z_r)^2}{2 P_b} \right] \\ &= 100 \times 1.1868 \times \frac{1}{1.9968} \left[\frac{0.1300 + 0.0605}{2 \times 0.3690} + \frac{0.0001 + 0.0151}{2 \times 0.3690} \right] \\ &= 16.55 \end{aligned}$$

Percentage of power loss: by using $\mu = 0.04$

$$\mu \Delta_2 = 0.04 \times 16.55 = 0.662 \%$$

Power loss based on power output

$$P_f = \frac{0.662}{100} \times 582,06 = 3.85 \text{ HP}$$

Total power loss due to gear tooth sliding:

$$\Sigma P_f = 4.23 + 3.85 = 8.08 \text{ HP}$$

(D) Windage and oil churning:

There are no direct information available with which to analyze the losses due to gear rotation in the media of air and atomized oil particles. For an approximation, it may be treated as the turbine disc rotating in the medium of wet steam. According to E. F. Church, Jr., "Steam Turbine" 3rd edition, McGraw Hill Book Co. Inc., 1950, the method is described on pp. 382.

Let the following items be considered analogous:

In turbine

In gear

Blade ring mean dia.

Pitch dia.

Blade height

Whole depth of tooth

Blade velocity

Pitch line velocity

The equation is

$$H = mn \left(\frac{U}{100} \right)^3 \frac{d}{V} \left[\frac{d}{2360} + \frac{C h_t^{1.5}}{26} \right] \quad \text{HP.}$$

where $m = 1.4$ for air and oil mixture (taken approx.

as same as wet steam)

$n = 0.25$ for large shielding and clearance.

U = pitch line velocity, fps.

V = specific volume of media, use $V = 16.7 \text{ ft}^3/\text{lb. (air)}$

at average temperature $\mathcal{F} = \frac{150 + 256}{2} = 203^\circ\text{F.}$

d = pitch diameter, in.

$C = 1$, constant treated as single row blade.

h_t = whole depth of tooth.

Then

$$H = 0.35 \left(\frac{U}{100} \right)^3 \frac{d}{16.7} \left[\frac{d}{2360} + \frac{h_t^{1.5}}{26} \right] \quad \text{HP.}$$

Tabulation of results

Rotating piece	Pitch dia. D or d , in.	Whole depth h_t , in.	Pitch Line velocity U , fps.	Power Loss H , HP.
Low-speed				
Gear	9.667	0.3917	190	0.02
Pinion	3.833	0.3917	190	0.01
High-speed				
Gear	11.375	0.2938	826	1.47
Pinion	2.125	0.2938	826	0.94
			Total	2.44

thesT823

A study of friction loss for spur gear t



3 2768 001 88853 0
DUDLEY KNOX LIBRARY